Archaeological and Anthropological Sciences (2021) 13:65
https://doi.org/10.1007/s12520-021-01303-6

ORIGINAL PAPER

Dragged, lagged, or undisturbed: reassessing the autochthony of the *hominin*-bearing assemblages at Gran Dolina (Atapuerca, Spain)

Palmira Saladié[1,2,3] · Antonio Rodríguez-Hidalgo[1,4,5] · Manuel Domínguez-Rodrigo[5,6] · Josep Vallverdú[1,2,3] · Marina Mosquera[1,2] · Andreu Ollé[1,2] · Rosa Huguet[1,2,3] · Isabel Cáceres[1,2] · Juan Luis Arsuaga[7,8] · José M Bermúdez de Castro[9] · Eudald Carbonell[1,2]

Received: 18 November 2020 / Accepted: 16 February 2021

Abstract

The TD6 unit of the Gran Dolina contains an assemblage of the Early Pleistocene, interpreted firstly as a home base. More recently has been proposed a transported origin of the remains according to the sedimentology. Following this model, the remains should be dragged or lagged in a predictable pattern related to their weight, density, shape, and size. Conversely, the debris generated in an undisturbed residential camp should retain spatial relations of codependence caused by the depositional process, not related to inherent variables of materials. To check if the remains were recovered in their original depositional place (aggregated) or are the product of transportation (segregated or random spatial relation), we have evaluated different variables: the spatial arrangement between osteological and lithic tools; the integrity of the bones and their structural characters (shape and tissue composition); postdepositional modifications; and the specimen size distribution. The combined results indicate that the layers that conform the TD6.2 subunit were undisturbed, while TD6.1 was affected by postdepositional processes, probably water flows, resulting in a lagged assemblage. In conclusion, TD6.2 is best interpreted as a well-preserved home base and should play a key role in studies of the behavior of the first European populations.

Keywords Spatial statistics · Water flows · Taphonomy · Bone integrity · TD6 unit

Introduction

The key to understanding a site is to comprehend how the archaeological record is formed, considering its previous existence in a systemic context (Schiffer 1983, 1987). All elements that enter into a cultural system are modified, decomposed, combined with others, used, and abandoned. LaMotta and Schiffer (1999) argued that the formation processes of the archaeological record can be summarized in three phases: (1) occupation/use; (2) abandonment; and (3) post-

✉ Palmira Saladié
psaladie@iphes.cat

✉ Antonio Rodríguez-Hidalgo
ajrh78@gmail.com

1 Institut Català de Paleoecologia Humana i Evolució Social (IPHES-CERCA), Campus Sescelades URV (Edifici W3), Zona Educacional 4, 43007 Tarragona, Spain

2 Departament d'Història i Història de l'Art, Universitat Rovira i Virgili, Avinguda de Catalunya 35, 43002 Tarragona, Spain

3 Departamento de Paleobiologia, Museo Nacional de Ciencias Naturales, C/José Gutierrez Abazcal, 2, 28006 Madrid, Spain

4 Department of Prehistory, Ancient History and Archaeology, Complutense University of Madrid, C/Prof. Aranguren s/n, 28040 Madrid, Spain

5 Institute of Evolution in Africa (IDEA), C/ Covarrubias 36, 28010 Madrid, Spain

6 Departamento de Historia, Universidad de Alcalá de Henares, Pza. San Diego, s/n, 28801 Alcalá de Henares, Spain

7 Centro Mixto UCM-ISCIII de Evolución y Comportamiento Humanos, C/Monforte de Lemos, 5, 28029 Madrid, Spain

8 Departamento de Paleontología, Universidad Complutense de Madrid, C/Prof. Aranguren s/n, 28040 Madrid, Spain

9 National Research Center on Human Evolution (CENIEH), Paseo Sierra de Atapuerca, 3, 09002 Burgos, Spain

Published online: 21 March 2021

abandonment. There may be accumulation processes in all these phases, that is, processes that incorporate materials into the assemblage and reduction processes that remove objects from the assemblage (Jiménez-Jáimez 2008). Knowing how items were transported and accumulated is an unavoidable issue if we want to reach some level of understanding of the archaeological assemblages, be it ecological, behavioral, or both. Aspects of human behavior in sites created by hominins and subsequently unmodified must not be interpreted at the same level of understanding as those assemblages that have been highly disturbed by other processes, generating new archaeological and/or taphonomic associations. It is essential to try to understand beforehand how the original assemblages may have been affected.

Transport and accumulation of bones from the place of death to the place of final deposition may be the product of different actors and processes. In this sense, the product of water flows has been considered one of the most powerful processes in the formation of fossil accumulations (Shipman 1981; Isaac 1983; Shipman and Rose 1983) and so it has long been studied (e.g., Voorhies 1969; Dodson 1973; Behrensmeyer 1975, 1988; Boaz and Behrensmeyer 1976; Petraglia and Potts 1994; Aslan and Behrensmeyer 1996; Coard 1999; Giusti et al. 2019). However, it is currently accepted that bones and teeth disperse as a function of differential transport according to their structural characteristics (Rogers and Kidwell 2007; Domínguez-Rodrigo et al. 2014, 2018, 2019b).

One of the pioneering works on the transport effect and drag produced by water flows on bone samples was the experiment conducted by Voorhies (1969). Through his observations, he divided the skeletal elements into three groups to predict the order of transport and dispersion. The distribution of elements within these groups may indicate the relative importance of the physical characteristics of the bones for their scattering. These characteristics are size, density, and shape, as for any other sedimentary particle (Behrensmeyer 1975). Aslan and Behrensmeyer (1996) also proposed differences in transport according to the weight of the bones. Coard (1999) supported these observations since he noted that the speed at which the bones are transported is related to a series of attributes, such as shape, weight, volume, and density.

More recently, Domínguez-Rodrigo et al. (2018) experimented on fluvial transport of bones of a recreated archaeological assemblage, subject to taphonomic alteration of both low-energy and high-energy water flows. In the statistical analysis of the samples, they considered three structural variables of the specimens: anatomical portion (axial skeleton, long bone epiphyses, and shafts); the shape of the bones (flat, tube, or cube) according to the relationship of their three-dimensional axes; and bone structure (cancellous, dense, and mixed). Results indicated the loss of most of the original spatial taphonomic associations of the original samples and the metamorphosis of the surviving association. Both experiments showed that diaphyses and epiphyses preserved an aggregative relationship. Axial bones suffered of higher rates of transport, being segregated from dense bones.

Petraglia and Potts (1994) observed that stone tools are dragged by water flow according to their weight, showing that groups containing more elements of larger sizes (so more weight) were more affected than others. According to this, lithic artifacts in lag contexts were in the same location where they were deposited by hominins, although there may be a slight loss of minor objects. Other types of materials originally deposited in locus (take as a synonym for undisturbed) were not present, which would point to segregation between lithic tools and other materials such as bones and teeth. Two scenarios can be considered regarding the transported lithic assemblages: (1) scattering of artifacts and (2) new concentrations of transported objects, modified concerning the original associations. This may involve scattering by size, emphasizing that larger objects will be closer and smaller ones further away from the original place of discard by hominins (Schick 1986; Schick 1987).

These studies noted that flows, whether of high or low intensity, affect archaeological remains according to their weight, structure, density, and shape. This leads to the segregation of materials according to these characteristics in the lagged or dragged assemblages. Therefore, it is expected that anthropogenic assemblages, in which the remains of the lithic tools and bones are deposited together, once affected by the water flow, will show biases from the original assemblages, with loss of their structural characteristics and their original spatial properties.

Commonly, accumulations in Pleistocene cave sediments are produced by natural deaths of animals, the activity of predators (including humans), and water flows, all of which may be also influenced by gravitational processes. Sierra de Atapuerca (Burgos, Spain) is rich in cave beds of archaeopalaeontological remains dated between the Early Pleistocene and the Holocene. Among the sedimentary units dated to the late Early Pleistocene, TD6 from Gran Dolina cave is the richest in the number of remains.

A description of the sedimentary facies of Unit TD6 at Gran Dolina (Campaña et al. 2016) has suggested that hominins, other animals, and lithic remains were mostly accumulated in the cave by geological processes related to channel and debris flows. According to this hypothesis, the remains would come from the adjacent slope above the cave or the cave entry. In this scenario, the remains accumulated in Unit TD6 would be in a secondary position, thereby reflecting a dragged assemblage. This implies that some of the inferences made previously regarding the behavior of the hominins that occupied the cave were wrong—particularly those that referred to the value of the microstratigraphic record of archaeopalaeontological assemblages (Canals et al. 2003a; Saladié et al. 2014) and, by extension, the behavioral interpretations—according to which TD6 was reconstructed as series of living floors.

Recently, Parés et al. (2020) have noted no signs of post-depositional disturbance or massive transport based on the magnetic susceptibility axes distribution in this unit. Besides, the results of Mosquera et al. (2018) had also defended the in locus character of the remains, given that "chaînes opératoires" in all raw materials are complete—meaning that all the products of each knapping stage are represented, and 12 groups of lithic refits belonging to knapping sequences and knapping accidents are present. Previous taphonomic works also support the undisturbed character of the association (Saladié et al. 2011, 2014). In this paper, our objective is to test the dragged, lagged, or undisturbed character of the TD6 remains through spatial statistics, postdepositional modifications, and the composition of the osteological elements according to their shape and structure, two variables which in turn correlate with the material's density, always intending to accept or reject the interpretations related to human behavior registered in TD6 unit.

The Gran Dolina site and the TD6 unit

Gran Dolina is located in the Railway Trench of Sierra de Atapuerca (Burgos, Spain). Eleven stratigraphic units were initially identified from bottom to top (TD1–TD11) (Gil and Hoyos 1987; Parés and Pérez-González 1995, 1999; Pérez-González et al. 2001), and then subsequently revised (Campaña et al. 2017; Rodríguez-Gómez et al. 2017; Parés et al. 2018) (Fig. 1b). Magnetic polarity dating has situated Unit TD6 in the Matuyama Chron (>780 ka) (Parés and Pérez-González 1995, 1999). Combined with electron spin resonance and uranium series, these results show an age of between 780 and 857 ka (Falguères et al. 1999). The more recent thermoluminescence and infrared stimulated luminescence data suggest an age of 960 ± 120 ka (Berger et al. 2008). Several stratigraphic studies have established that Unit TD6 of Gran Dolina dates to the late Early Pleistocene (Parés and Pérez-González 1995, 1999; Falguères et al. 1999; Pérez-González et al. 2001; Berger et al. 2008; Parés et al. 2013). In addition, direct ESR dating on a *Homo antecessor* tooth (ATD6-92) supports an age between 772 and 949 ka (Fig. 1), in agreement with previous dating studies (Parés et al. 2018).

Almost 20 m^2 of the TD6 surface have been excavated in two phases. The first phase between 1994 and 1997 involved the excavation of a test pit (Fig. 2a). This excavation affected about 6 m^2, in which abundant hominin remains, fauna, and lithic tools appeared (Carbonell et al. 1999a). The excavation of the sedimentary portions overhanging the Gran Dolina section, also involving TD6, began in 2003 and finished in 2011. These works affected a surface of around 12 m^2. It entailed the so-called Torreón and the central area (Fig. 2a). In both areas, abundant archaeological remains were documented in agreement with the sample recovered in the previous period of TD6 excavation (test pit). TD6 is a 3-m-thick unit divided into three subunits, from bottom to top: TD6.3, TD6.2, and TD6.1. TD6.3 contains the least anthropic impact. Subunits TD6.2 and TD6.1 show the most intense anthropic activity, as demonstrated by the analyses of both stone tools and bones with anthropogenic modifications (Fernández-Jalvo et al. 1996; Díez et al. 1999; Saladié 2009; Saladié et al. 2011, 2012, 2014, 2019; Mosquera et al. 2018). These last two subunits are the focus of this paper.

Taphonomic and technological data (Carbonell et al. 1999b; Díez et al. 1999; Saladié et al. 2011, 2014; Mosquera et al. 2018) suggested that hominins played the central role in the formation of the faunal assemblage of TD6.2. There is less data for TD6.1, so we will start from the hypothesis that its composition is consistent with TD6.2. TD6.1 was identified in the central area and the test pit. However, it is absent in the "Torreón" area. A high presence of coprolites characterizes the test pit and part of the central area for TD6.1. During the enlargement of the excavation surface, a marked change was observed regarding the composition of the archaeological materials, characterized by lithic remains and faunal and hominin specimens with carnivore and anthropogenic modifications, which were recovered in the central area of the TD6.1 surface.

Lithostratigraphic descriptions, carried out at the end of the 1980s, considered the deposits of TD6 as a rockfall deposit with limestone boulder and gravel formed by gelivation and non-channelized water flows (Hoyos and Aguirre, 1995). After the discovery of *Homo antecessor* in the test pit area, the Aurora stratum was defined as a stratigraphic marker. The Aurora stratum comprised a homogeneous muddy-supported boulder breccia of 0.20 m in thickness (Parés and Pérez-González 1999). The muddy matrix contained massive lutites with clasts larger than 22 cm (boulder). According to Parés and Pérez-González (1999: Fig. 6), a deposit of calcarenites marks the top of the *Aurora stratum*, and a downfall clast deposit delimits its base. A few years later, the description of the sedimentary microfacies and soils micromorphology of the *Aurora stratum* and archaeostratigraphical research based on the archaeological and palaeontological record of the test pit excavations indicated that the archaeological remains of the Aurora stratum were a microstratified assemblage deposited in a nonhomogeneous stratum (Vallverdú et al. 2001; Canals et al. 2003b).

The microstratified character of the archaeopalaeontological assemblage of the Aurora stratum was confirmed in the stratigraphical observations based on the TD6 central section of Gran Dolina (Bermúdez de Castro et al. 2008). In this part, the thickness of the *Aurora stratum* reaches 0.46 m and is described as a lithologic sequence of at least six layers of fine gravels, sands, and muds. Incorrectly, all human remains were originally attributed to the *Aurora stratum* in the first works

(Carbonell et al. 1999a). Current research has shown that *H. antecessor* specimens occurred along the several layers of TD6.1 and TD6.2 (Bermúdez de Castro et al. 2008; Carbonell et al. 2010; Saladié et al. 2014). The last research of the sedimentary facies of TD6 (Campaña et al. 2016) suggested that sediment gravity flows and water flows (channel, flood plain, and decantation) were the primary mechanisms for the accumulation of the remains from allochthonous deposits to Gran Dolina. However, the sedimentary infillings by rockfall from the roof of the cave, acting as a cliff, can be considered an alternative sedimentary model for guiding the description and interpretation of the TD6 and, in general, Gran Dolina sedimentary succession. The diamictons, debris flow facies described in Campaña et al. (2016), are common sedimentary facies in the caves' interior. However, we regard cave entrances and rock shelters as a different depositional environment (Ford and Williams 2007). The current cave entrance points of Gran Dolina are located in its roof, in the form of ponor (avens or shafts). The cliff's slow backward movement provides the primary rockfall deposits in talus slopes (Luckman 2013), the classical analogy with the escarpment that provides the sedimentary material that feeds deposits at the feet of rock shelters and cave entrances.

The TD6.2 bedset in the central part of the Gran Dolina (SOM Fig. S1) infill lies on a scoured surface, the upper surface boundary of the subunit TD6.3.1, and truncate a massive mud-supported boulder breccia bedset of TD6.2 located below the SE cave wall. This central part of the TD6.2 bedset contains an inclined and cemented microstratification made from coarse and fine gravels and outsized boulders, in openwork, to clast-supported gravel with yellow-brown sands. This scour infilling of the TD6.2 is interbedded to the NW with a microstratified horizontal bedset of microbreccias. This microbreccia bedset of the central part of TD6.2 contains

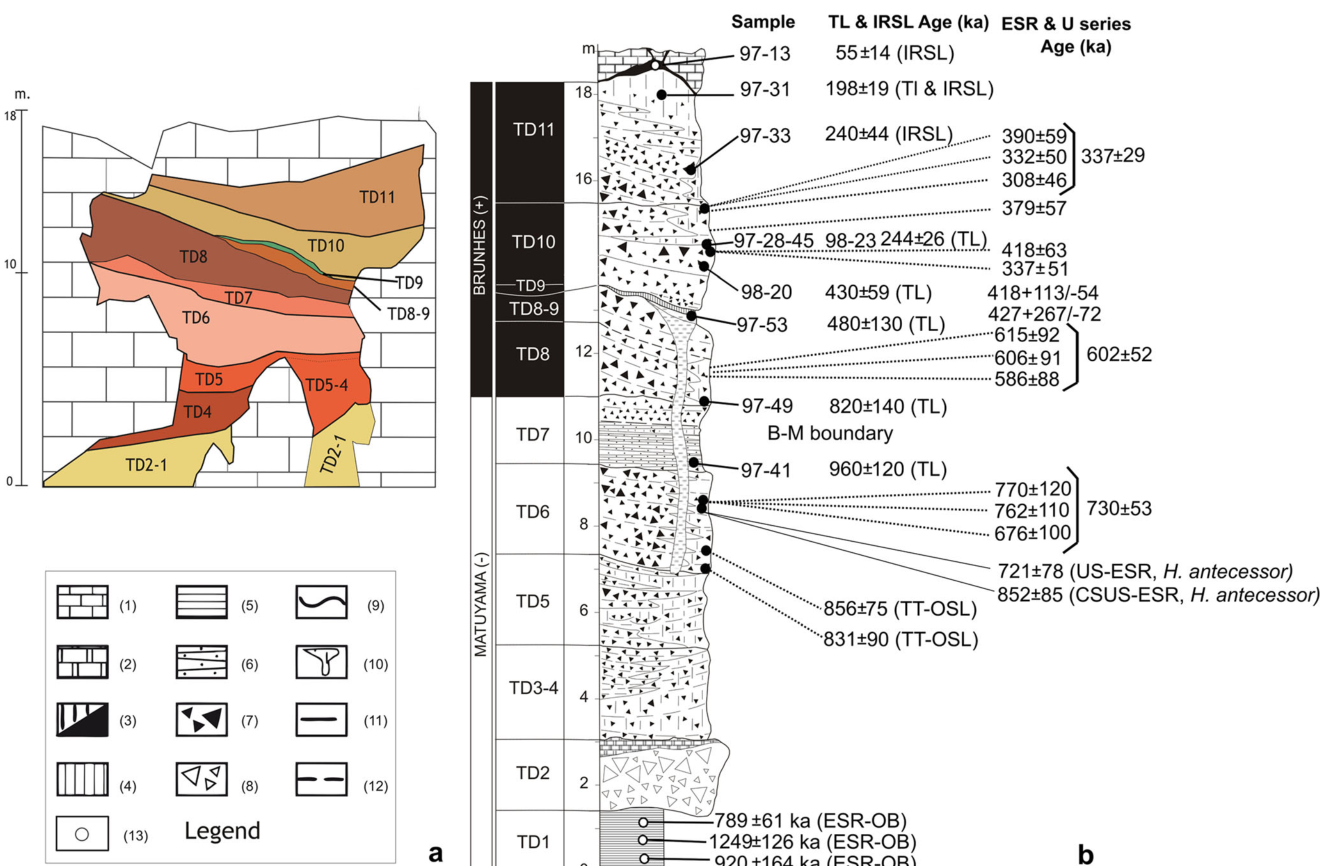

Fig. 1 **a** Stratigraphic section of the Gran Dolina site. **b** Synthetic stratigraphic profile with the locations of the available TT-OSL, TL, IRSL, and ESR/UTh dates from Falguères et al. (1999, 2013), Berger et al. (2008), Arnold et al. (2015) and Duval et al. (2018). Legend: 1 = Mesozoic limestone at the roof of Gran Dolina; 2 = speleothem; 3 = lutites, clay loam/terra rossa; 4 = bat guano; 5 = laminated loamy clays; 6 = calcilutites and calcarenites; 7 = gravels and boulders, clastic flow; 8 = arrangement of fallen boulders; 9 = main stratigraphic discontinuity; 10 = secondary unconformity and loamy-clayey-sandy filling; 11 = Matuyama-Brunhes boundary; 12 = disappearance of *Mimomys savini* and first occurrence of *Iberomys brecciensis*; 13 = location of the *Aurora stratum* (containing the hominin remains) at the top of TD6 (modified from Berger et al. 2008)

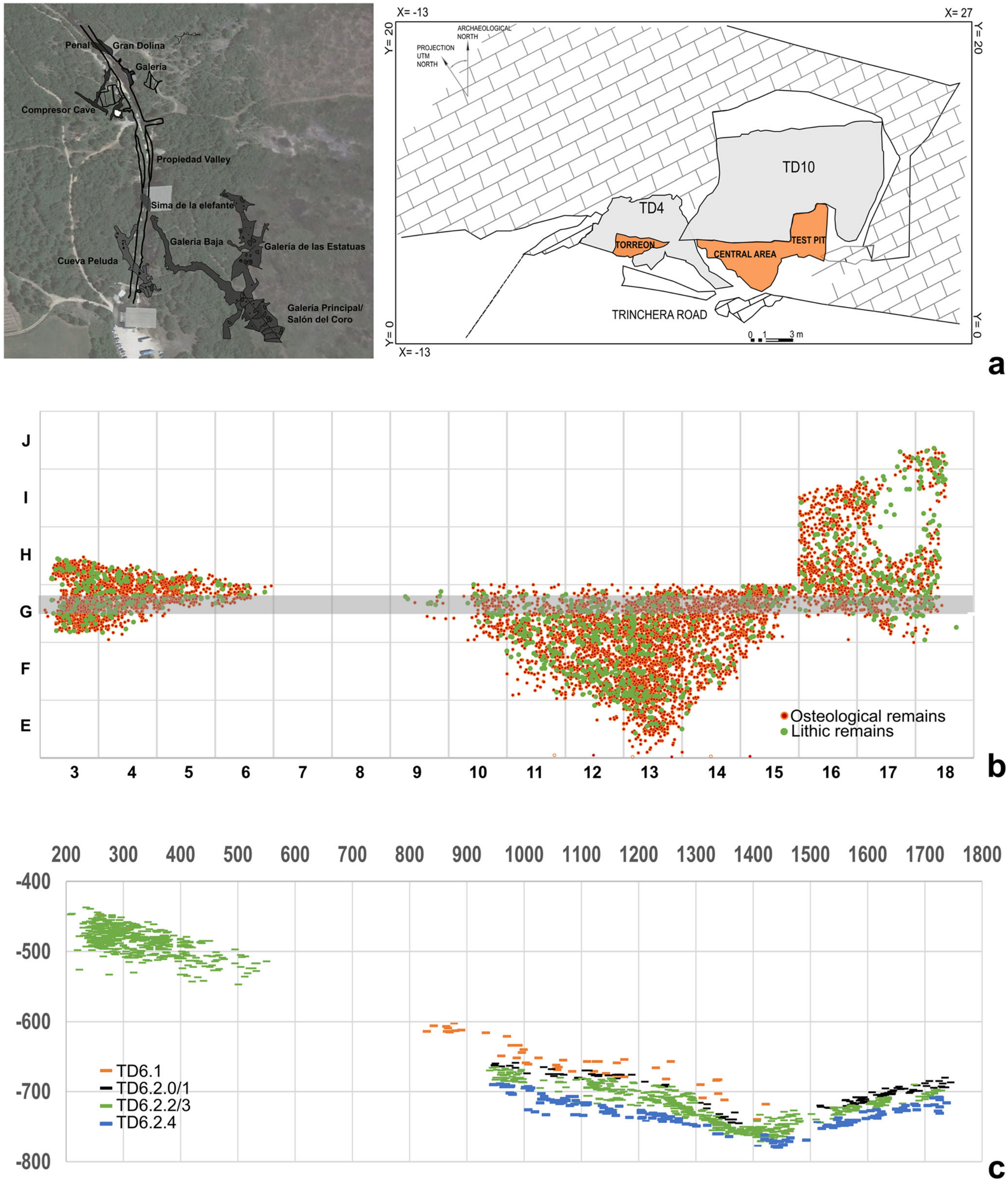

Fig. 2 **a** Scheme of the location of the sites located in the Trinchera del Ferrocarril in the Sierra de Atapuerca. **b** Horizontal plot of the osteological and lithic remains from TD6.1 and TD6.2. **c** The projection of materials corresponds to 20 cm from squares G line (650–670 cm of absolute coordinates of the Y axis in the horizontal plane of surface)

rhythms (Vallverdú et al. 2001) of poorly sorted fine gravels, in openwork to clast-supported fabrics and yellow-brown sands. The yellow-brown sands are massive, graded, and laminated. The rhythmic microstratification has limited lateral and vertical accretion by its centimetric thickness. The mud-supported boulder breccia located in the SE cave wall forms coarse prismatic secondary aggregates and contains graded lamina fragments as mud clast. To the NW cave wall, the microstratified deposits of the central part of Aurora stratum are interbedded with two unstratified deposits made from very inclined gravel and yellow-red muddy sand breccia. These two bedsets show a typical fall sorting of the gravels (coarse tails) from fine to coarse gravel sizes (Hétu 2004).

The lower surface boundary of the microstratified microbreccia bedset, at the center stratigraphic panel of TD6.2, onlaps the upper surface boundary of this first inclined bedset above the NW cave wall. At the other lateral termination, the lower surface boundary of the second bedset of breccia inclined above the NW cave wall downlaps the upper surface of the microstratified microbreccia. This depositional geometry between bedset of NW and central profiles offers a rich analogy with the "downlap interval" described in Quaternary talus slope successions (Sanders et al. 2009).

In our opinion, the interpretation of TD6.2 is related to the backward retreat of the entrance point of the roof escarpment of the NW wall of the Gran Dolina cave. The feet of the talus slope show changes in its morphology and sedimentary processes too. These changes are indicated by the truncations of the upper surface of TD6.3.1. The talus slope's modifications by fluvial incisions suggest a talus cone morphology also typical in the cave entrance setting. The retreat of the cave escarpment likely was accompanied by the development of the rills' hierarchy and changes in the sediment of the source area at the outer slope (exocarstic) cave setting. The poor and inclined stratification with outsized boulders infilling, in the main scour surface of the lower surface boundary at the center of the TD6.2 profile, points to colluvial sediments set in an abandoned rill (scour and fill). The fluvial incision over the cave entrance's talus slope can be considered limited by the scours' size in the top of the TD6.3 boundary surface. The description of the rhythms of beds made from microbreccias and yellow-brown sands in horizontal stratification (Vallverdú et al. 2001) implies at least four types of different deposits. Fine gravel beds of one or two lines of fine gravel with sand support (1), sorted fine gravels grading to sand (2), matrix support or cemented openwork (sieve deposit) (3), and coarse bed of fine gravels in clast support fabric (thick bed load) (4) show the transition from low-density to high-density (traction carpet) water flows (Todd 1996). Fine gravel with sand shows coarse tail grading points to subaquatic mass sedimentation (Nemec and Steel 1984). Openwork fabric of fine- or clast-supported gravels suggests emersion of levee deposits formation. The flooding of the foot of the cave sedimentary infilling close to the NW wall of Gran Dolina, due to episodic currents, is also indicated by the fragmented graded lamina (aggregate soft clasts) within the prismatic mud of the boulder breccia of SE cave wall pointing out sheetwash deposits widely described in the archaeological cave entrance and rock shelter settings, infilling openwork rockfall deposits (Lenoble 2016). The episodic subaquatic sedimentary process, interpreted in the central area of TD6.2 profile, suggests that there was likely an ephemeral body of water in the cave entrance of Gran Dolina.

TD6.1 lies on a weathered surface, observed across the central area and SE pit test over the top of TD6.2, which was described as a calcarenite bed in previous stratigraphic observations in the Test pit area (Parés and Pérez-González 1999). The top of TD6.1 is the erosive unconformity that separates the lithostratigraphic units TD6 of TD7. The lateral and vertical changes of the deposits of TD6.1 are like that of TD6.2. TD6.1 has a scour attached to the inclined breccia of the NW wall. Above the NE cave wall, this inclined stratification of the breccia bedset contains subvertical boulders and has a convex form and truncated upper surface boundary. The lower surface boundary of the NW breccia lies on downlap over the bedsets of the central area profile. These sedimentary deposits of the central part of TD6.1 are made from sorted fine and medium gravels poorly stratified in concave bedforms with openwork and clast-supported fabrics. In the lower part of the slope of the central area of TD6.1, the concave and horizontal geometries of the bedsets are amalgamated and truncated. The boulder set in prismatic muddy-supported breccia, close to the SE cave wall, presents 0.25 m thick above the previously described calcarenite bed of the top of TD6.2 (Parés and Pérez-González 1999)

The interpretation of TD6.1 shows the talus cone's progradation of the cave entrance to the interior of the cave. The NW stratigraphic profile of the test pit shows the lower surface TD6.1 bedset downlap in proximity to the upper surface boundary of TD6.3.1 (Vallverdú et al. 2001). The sediments at the entrance point into the vertical escarpment continue their backward retreat and likely increase the rill catchment area in the outer exokarstic slope. Limestone sorting and amalgamated and truncated scours described in the central area of TD6.1 indicate proximal fluvial incisions typical of the talus cone morphology in the entrance cave. Openwork and clast-supported fabric suggest the participation of water and granular flows. Large boulders, of outsize measures, set in subvertical position in the top of the upper and convex surface boundary of the breccia bedset, located above the NE wall, indicate a preliminary interpretation based on sedimentary processes described as boulder rockfall over snow or ice (Luckman 2013).

Materials and methods

The excavation of TD6 was conducted using Cartesian coordinates on a grid of 1 m^2. All-natural cobbles and boulders of limestone larger than 10 cm were recorded, as well as each lithic and bone specimen, regardless of the size. Bearing and plunge were recorded with respect to the archaeological north. Bearing is the horizontal angle of the long axis line relative to some geographic or arbitrary north, and the plunge is the vertical angle of the line relative to the horizontal plane (McPherron 2018). The objects with a plunge angled of 0 were described as flat, and the objects with a plunge angled of 90 were described as verticals. We offer the data of the elongated specimens (with lengths at least twice the widths). During the excavation, the remains were ascribed to subunits TD6.1 or TD6.2. Mosquera et al. (2018) have been able to divide subunit TD6.2 into three archaeological groups of layers, which they call (from bottom to top), and following the facies described by Campaña et al. (2016): TD6.2.4, TD6.2.2/3, and TD6.2.0-1. This partition is the most congruent in the vertical distribution of the remains. It therefore is the one we will follow in this work to apply statistical tests and archaeological and taphonomic analyses (Fig. 2c).

A total of 7972 remains have been recovered in subunits TD6.2 and TD6.1. The dimensions of the archaeological remains are given in frequencies. Considering that about 94% of the objects measure less than 9 cm (93.1% of the bones and 95% of the stone tools), we decided to group them into categories of 3 cm. Layer TD6.2.2/3 has the greatest number of remains and TD6.1 the least. In the spatial analysis, it included all remains from which spatial coordinates were taken (Table 1). The osteological sample refers to bones and teeth of fauna, hominins, and indeterminate specimens. A general description of the assemblages is done. For bone description, we use the division of the limbs in three parts (Domínguez-Rodrigo 1997): upper (humerus and femur), intermediate (radius and tibia), and distal (metapodials). We offer the number of specimens (NSP); number of identified specimens (NISP); minimal number of elements (MNE), and the minimal number of individuals (MNI).

The point pattern analysis of the archaeopalaeontological remains from TD6.1 and TD6.2 subunits of Gran Dolina has been evaluated, within the perspective of spatial taphonomy defined as the study of the spatial distribution patterns of the archaeological remains in relation to their taphonomic attributes (Domínguez-Rodrigo et al. 2018). These analyses are useful for assessing the deposit processes and the integrity of the archaeological assemblages and for a reliable interpretation of past human behaviors (Giusti et al., 2018). The spatial properties of archaeopalaeontological assemblages may contain high information concerning the biostratinomic phase, such it is indicated by the referential frameworks (Domínguez-Rodrigo et al. 2018). The spatial statistical tools to the sites are used to know if the assemblages have been reworked or are in situ (Giusti and Azzarello 2016), to assess the impact of water on any archaeofaunal assemblage (Domínguez-Rodrigo et al. 2018), to know the spatial relationship of dependence or independence between fauna and lithic tools and debris (Giusti and Azzarelo, 2016; Giusti et al. 2019), and also to infer aspects about the socioeconomic organization of early humans in assemblages through the observed spatial organization (Domínguez-Rodrigo and Cobo-Sánchez 2017), or even to separate different occupations through their spatial independence and taphonomic properties (Marín et al., 2019). We start from the fact that objects in space can be distributed and related to each other in three ways:

1. Distribution of grouping—it is considered that the specimens are grouped in space for what underlies a dependency relationship.
2. Regular dispersal—the remains are regularly separated from each other, which can also mean a dependency relationship
3. Random distribution—Poisson process by which there is no spatial relationship between objects. This can be interpreted as that there may have been depositional processes that have affected the existing spatial relationships between objects in their original position.

We used Spatstat package v. 3.2.3 (Baddeley et al. 2015) in R (R Core Team, 2018) for the statistical spatial analysis. To assess the distribution of the objects and their spatial attributes in TD6.2.2/3, we have built two independent windows. On the one hand, it was considered the test pit and the central area. On the other was drawn the "Torreón" area in order to avoid false statistical artifacts related to a nonexistent empty space (Fig. 1b). The "Torreón" area has not been analyzed for the other layers because of the absence of TD6.1 and TD6.2.0/1 there and only has a few objects in TD6.2.4.

A nonparametric method of Kernel maps was also used to produce graphic smoothing estimations of intensity. Density maps were made by using bandwidths selected by sigma values, which control the degree of smoothing. Corrections for window-edge effects were considered in all mapping methods. To select the optimal bandwidth, Diggle and

Table 1 Number of osteological remains and lithic pieces recovered in TD6.2 and TD6.1 subunits

Subunit	Layer	Osteological sample	Lithic sample	Total
TD6.2	TD6.2.4	594	236	830
	TD6.2.2/3	4732	388	5120
	TD6.2.0/1	1089	207	1296
	Total	6415	831	7246
TD6.1		602	124	726
Total		7017	955	7972

In the table are presented the layers that are considered in this study

Berman's mean square error cross-validation method and the likelihood cross-validation method were used (Berman and Diggle 1989). Diggle's correction is commonly used to minimize the edge effect, but it assumes a Cox clustering process (Baddeley et al. 2015), which in the present case is inadequate. For this reason, we selected a likelihood cross-validation algorithm that assumes an inhomogeneous process as shown by homogeneity tests. Clustering was approached through Clark-Evans tests using Monte Carlo simulations (n=300). This test produces R values from 0 (confirmation of the null hypothesis of theoretical complete spatial randomness (CSR)) to 1 (maximum cluster). However, this test assumes homogeneity and can be biased in inhomogeneous point processes. As a complement, the Hopkins-Skellam test was also used because it is less sensitive than the Clark-Evans test to inhomogeneity (Baddeley et al. 2015). This test produces a value of A, which indicates a random pattern (A=1), clustering (A<1), and regularity (A>1). The test was also performed using a Monte Carlo simulation.

Lithics and osteological elements from TD6.2 and TD6.1 were considered independently in order to evaluate the spatial patterns of distributions. We used Ripley's K functions (Ripley 1976, 1977, 1979). The K function measures the cumulative average number of points falling within a certain radius of any given data point. This estimation is corrected for window-edge effects and modified according to intensity. However, the K function operates under the assumption that the point process is homogeneous, and alternative, more robust modified versions of this test exist. L function can adopt a centered version of the K function and applies a square root transformation of the Poisson K function. This stabilizes the variance (Ripley 1979). We used the quadrat counting (chi-squared) test of homogeneity by dividing the spatial window into square meter subunits. The quadrat test was executed via Monte Carlo (Robert and Casella 2004) simulations (n = 300), and the result was obtained by averaging all simulations. According to the results (Supplementary Online Material [SOM] Table S1), we have applied the inhomogeneous version of L functions. Acceptance intervals were obtained via a Monte Carlo simulation process involving 50 random samplings of the original data (Baddeley 2015). These functions are used to describe how a point process occurs in any specified spatial window when the spatial point pattern is nonstationary. The curve of the observed data was interpreted as showing an aggregation process of objects (above CSR line), a regular dispersion process of objects (under the theoretical CSR line), or complete spatial randomness (if within the confidence intervals of the CSR line).

After the independent evaluation of lithic and osteological samples, a cross-type approach was implemented to study the point patterns by material type. The multitype pattern was oriented to detect spatial codependence between lithic and osteological remains; archaeological remains and clasts limestones; and fauna and *H. antecessor* specimens in TD6.2.2/3 since it is the layer with the greatest number of remains. For this purpose, an inhomogeneous cross-type L function was used (Ripley 1979). The multitype summary functions are used in the analysis of the dependence between points of the samples. The L_{ij} indicates the association between osteological and lithic samples. If the data line is outside the confidence acceptance, then both types of materials are spatially dependent. This can be expressed by being clustered (the probability of i points being within the distance of any specific radius of j points is higher than the benchmark value), or regularly spaced (the probability of i points being within the distance of any specific radius of j points is lower than the benchmark value). This analysis is displayed in a bivariable quadruple graph. The diagonal graphs (upper left and lower right) indicate the inhomogeneous L_{ii} distribution. The off-diagonal graphs (upper right and lower left) indicate the inhomogeneous L_{ij} association type. Global 95% confidence acceptance was used (Baddeley et al. 2015).

A positive spatial correlation between the two types of samples would suggest that the assemblages are found in associated spatial position, and so the null hypothesis of independence (CSR) can be rejected. The rejection of the null hypothesis could support that the different elements were not disturbed by flow taphonomic processes since these processes are disaggregates, not aggregators. The segregation of the two samples would point to variation in the distribution of types. Segregation could permit interpretation that the osteological and lithic samples were deposited in independent events or that they have been affected by secondary taphonomic processes. We assumed that a completely random spatial distribution of the lithic artifacts and faunal remains would suggest independence deposition events or re-elaboration of these materials.

For cross-type point comparison in postdepositional altered bones tested the complete spatial randomness and independence (CSRI). For this purpose, the multitype L function (L_{ij}(r)) was used (both for homogeneous processes). If $i = j$, then $L_{ij}(r) = L_{ii}(r)$; that is, it has the same interpretation as the regular L function regarding clustering, segregation, and randomness. However, if $i \neq j$, then Kij(r) measures the dependence between i and j point types. This dependence can be expressed in association or segregation (above the benchmark value). The benchmark value, which in the standard L function implies CSRI, implies point independence here (Ripley 1988). Confidence acceptance was selected via resampling (n = 50) Monte Carlo methods. CSRI was selected because it was hypothesized that every mark in the spatial point pattern would be independently and randomly distributed if transportation processes caused their accumulation from their original depositional locus. Transportation would break the interdependent depositional properties that functionally linked lithics and bones and their taphonomic properties as they were jointly deposited on the ground. These spatial functional and spatially interdependent properties would have been broken by resedimentation and allochthonous deposition.

Frequencies of postdepositional modifications are reported for each of the layers. Manganese oxide stains can exhibit a dendritic pattern or mask coatings (López-González et al. 2006). Weathering degrees are described according to Behrensmeyer (1978). Abrasion, trampling, sediment cementations, and cracks caused by changes in humidity have been recorded (Shipman 1981; Fiorillo 1984; Thompson et al. 2011; Fernández-Jalvo and Andrews 2016). The diversity of postdepositional modifications in TD6.2 and TD6.1 samples is high and they have different natures, although most of them are related to the possible presence of water flows, or embankments and humidity. Abrasion and trampling can be related to the movement of bones in the sediment. The aggregation of manganese oxide stains and cementations may suggest the presence of water on the surface once the remains are buried. The weathering supports those humidity changes, although it can also be related to the origin of the elements of environments with less radiation protection. The CRSI or segregation between the different modifications suggests that the actor responsible has not affected the assemblage samples in the same way. In this sense, postdepositional taphonomic processes could not be the accumulator's agents and we should reject the hypothesis that the studied samples are reworked.

Additionally, we evaluated the composition of the archaeological assemblages together with a sample coming from an undisturbed Masai Camp, an experimental lag set, and an experimental set transported at a maximum distance of 20 m (Domínguez-Rodrigo and Cobo-Sánchez 2017; Domínguez-Rodrigo et al. 2018, 2019a). The three samples are useful to assess the influence of water currents on a set and if its position is secondary (Domínguez-Rodrigo et al. 2019a). Currently, the referential frameworks for this analysis are still scarce and future implementations will undoubtedly be necessary to reinforce the established analogies. The validity of the analogy lies in the fact that we consider the immanent characters of the remains. The variables considered were bone shape and structure (Domínguez-Rodrigo et al. 2018). Bones organized by shape were divided into flat bones (composed mainly by shaft fragments, ribs, and scapulae, but also mandibular fragments); cube-shaped specimens (mainly vertebrae and carpal/tarsal bones); and tube-shaped bones (specimens mostly formed by epiphyses). Besides, it is very important to recognize that we do not have actualistic samples that allow us to evaluate an assemblage produced by a debris flow from the point of view of the shape and structure's composition. However, this proxy will be useful to evaluate if any of the analyzed assemblages are lagged or dragged, or on the contrary, remain in the deposition site according to these formal characteristics.

Results

TD6.2.4

TD6.2.4 forms the base of TD6.2 subunit. It has a lower density of specimens than the overlying sublayer (TD6.2.2/3). It was identified in the central area of the excavated surface and the test pit. In TD6.2.4, there were recovered 236 lithic tools. No preferential bearing of the objects is observed and 47.4% have a flat inclination (SOM Table S2). The sample is made up of hammerstones and hammerstone fragments and cores: tools made on cobbles, flakes, and retouched flakes (Mosquera et al. 2018). In this set, three groups of lithic refits formed by two pieces each were found. The refits are at distances ranging between 10 and 60 cm of one another. Two of them are products of the knapping process and the third is one Siret fracture (Mosquera et al. 2018: Table 8). The osteological sample comprises 594 remains, three specimens of *H. antecessor*, 118 faunal remains, and 473 indeterminate fragments (SOM Table S3). Up to 85.8% of bones and teeth and 80.7% of stone tools are less than 60 mm in maximum length, with the majority measuring less than 30 mm (Table 2). Remains larger than 60 mm are also present in the assemblage. The maximum lengths are measured from one quartzite hammerstone (170 mm) and one shaft of a large animal (160 mm).

Smoothing Kernel density maps of osteological and lithic remains showed spatial overlapping between both materials (SOM Fig. S2). This agrees with the result of Clark-Evans test which also showed substantial clustering for both. The Hopkins-Skellam tests coincide to show bone and lithic remains highly clustered (Table 3). However, the interpretation of the results must be nuanced. The inhomogeneous version of L tests suggested a random dispersion for bone remains up to 60 cm and slight clustering at longer distances (SOM Fig. S2c). This tendency toward regular dispersion was also documented in the case of stone tools, with slight clustering in distances >80 cm (SOM Fig. S2d). However, the relationship according to the multitype inhomogeneous L function showed a trend toward slight clustering beyond a 20 cm of distance. This points to a codependence in the form of clustering of lithics and bones after a 20 cm of distance from any random point (Fig. 3). However, the same test shows no spatial relation between archaeological remains and the clasts of the layer (SOM Fig. S3).

According to the structure and shape of the bones, the assemblage is characterized by the presence of dense and flat bones, mainly shaft fragments of long bones (Table 4, Fig. 4). The most common species in this layer are medium-sized cervids (*Dama dama vallonetensis*, *Cervus elaphus* cf. *acoronatus*; SOM Table S3). The other taxa include herbivorous and carnivorous species, but the NISP is scarce in all cases. The taxonomic diversity is homogeneous according to

Table 2 Distribution according to dimensions of the remains of TD6.2.4, TD6.2.2/3, TD6.2.0/1, and TD6.1

	TD6.2.4		TD6.2.2/3		TD6.2.0/1		TD6.1	
	Bones	Lithic tools	Bones	Lithic tools	Bones	Lithic tools	Bones	Lithic tools
<30 mm	52.7%	41.3%	49.7%	44%	48.3%	49.7%	38.2%	21%
31–60 mm	33.1%	39.4%	35.6%	40.7%	36.6%	25.4%	44.1%	53.1%
61–90 mm	9.6%	16.9%	9.4%	11.8%	10.2%	18.3%	12.7%	19.1%
>90 mm	4.6%	2.4%	5.3%	3.6%	5%	6.5%	5%	6.8%

the Shannon index (E = 0.6355), without any of the taxa standing out predominantly above others (Simpson index: D = 0.3366). A total of 4.7% of specimens with cut marks indicates a complete butchering process, 2.4% of bones show traces of percussion bone breakage, and 2.1% show peeling. In total, 9.1% of the remains of layer TD6.2.4 show at least one anthropogenic modification. Carnivore modifications are acid digestion corrosion (NSP = 10, 32.2%); pits and scores (NSP = 7, 22.8%); licking (NSP = 5, 16.1%); pitting (NSP = 1, 3.2%); and crenulated edges (NSP = 1, 3.2%).

The postdepositional modifications of the osteological set of TD6.2.4 are (SOM Table S4) manganese oxide stains (31.8%); sediment attached to bone surfaces (9.3%); humidity cracks (2.5%); abrasion (2.5%); trampling (1.6%); and weathering (0.5%). Manganese oxide stains exhibit a dendritic form (98.2%), mask coatings (1.4%), or both (1.4%). In most cases, a scattered pattern of stains is shown on the entire surface of the bones (96%). This includes fracture edges (dry and green), articular parts and areas of muscle insertions, and the rest of bone surfaces. In one case, secondary coating has been observed (after López-González et al. 2006). Abrasion produced by water flows on bones occurs in slight stages, affecting in all cases only the edges of fractures. Weathering is categorized as stage 1, according to Behrensmeyer's (1978) referential diagnosis.

Kernel density maps showed spatial overlapping between cemented bones, humidity cracks, and manganese oxide stains (Fig. 5a). This may be related to alternative periods of humidity and desiccation in this area. Weathering, abrasion, and trampling are scarce and do not show spatial overlapping, which does not support the inferences of reworking or reelaboration. Multitype L cross functions displayed at most of the postdepositional modifications show spatial clustering between them (Fig. 5b), although an exclusion model is observed between abrasion and weathering.

TD6.2.2/3

This is the most extensive layer of subunit TD6.2, which also contains the highest density of materials. The areas excavated of TD6.2.2/3 are the test pit, the central area, and the "Torreón." A total of 388 pieces make up the lithic sample, which is composed of cobbles, fragments of cobbles, hammerstones, cores, flakes, and retouched flakes. In this layer, four groups of lithic refits have been recorded. Refits were at a minimum distance of 5 cm and a maximum of 768 cm (Mosquera et al. 2018). A total of 913 faunal remains, 111 specimens of *H. antecessor*, and 3705 indeterminate bone fragments form the osteological sample (NSP = 4729).

Table 3 Values of the Clarke-Evans and Hopkins-Skellam tests (300 simulations) for clustering for osteological specimens, lithic tool pieces, and human remains of TD6.2.4, TD6.2.2/3, TD6.2.0/1, and TD6.1

	Bone (fauna and human remains)		Lithic tools		Human remains	
	Clark-Evans	Hopkins-Skellam	Clark-Evans	Hopkins-Skellam	Clark-Evans	Hopkins-Skellam
TD6.2.4	R = 0.78552	A = 0.054647	R = 0.79078	A = 0.19748	R = 1.9887	A = 9.3769
	p = 0.006645	*p < 2.2e-16*	*p = 0.006645*	*p < 2.2e-16*	*p = 0.7708*	*p = 0.01541*
TD6.2.2/3	R = 0.75735	A = 0.086931	R = 0.77269	A = 0.32527	R = 0.79453	A = 0.81384
	p = 0.006645	*p < 2.2e-16*	*p = 0.006645*	*p < 2.2e-16*	*p = 0.006645*	*p = 0.7053*
TD6.2.2/3 "Torreón"	R = 0.82705	A = 0.20807	R = 0.92343	A = 0.5242	R = 0.5436	A = 0.75824
	p = 0.006645	*p < 2.2e-16*	*p = 0.01993*	*p = 1.741e-09*	*p = 0.006645*	*p = 0.6116*
TD6.2.0/1	R = 0.75735	A = 0.13314	R = 0.77269	A = 0.1235	R = 0.65075	A = 1.305
	p = 0.006645	*p < 2.2e-16*	*p = 0.006645*	*p< 2.2e-16*	*p = 0.006645*	*p = 7 0.6252*
TD6.1	R = 0.87916	A = 0.30997	R = 0.86948	A = 0.3601	R = 1.1751	A = 1.0079
	p = 0.006645	*p < 2.2e-16*	*p = 0.006645*	*p = 2.765e-15*	*p = 0.8771*	*p = 0.9885*

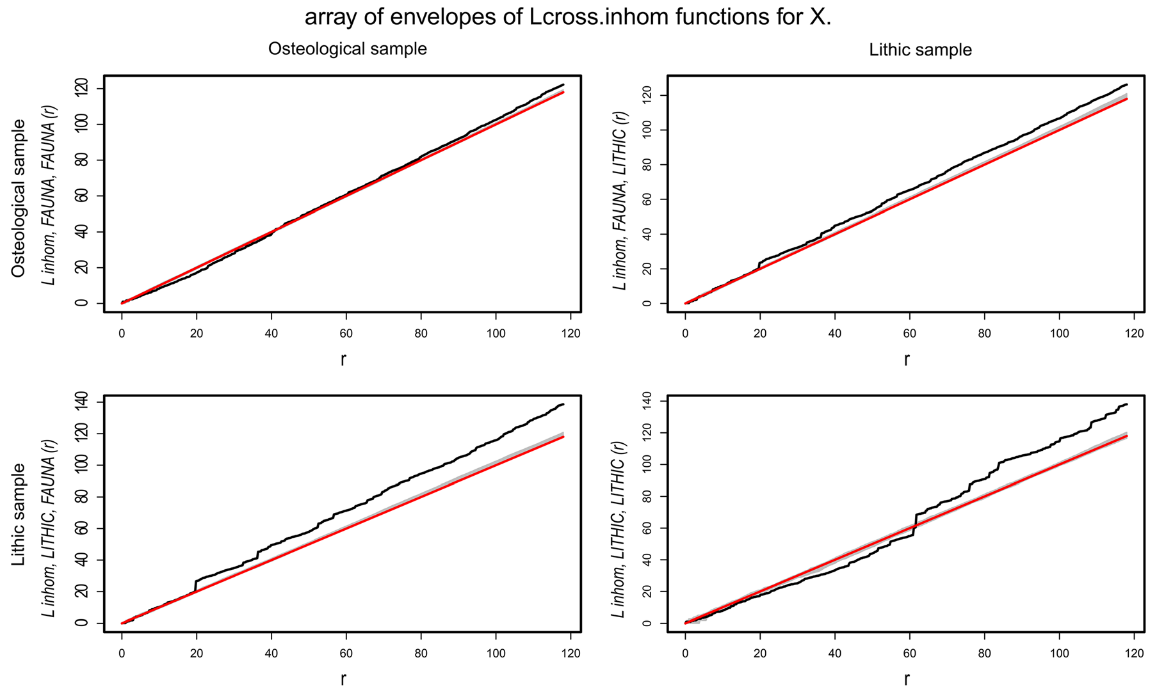

Fig. 3 Multitype inhomogeneous L function for osteological and lithic remains from TD6.2.4 at the central and the test pit areas

Specimens smaller than 30 mm are the most abundant in the assemblage, similar to those between 30 and 60 mm (Table 2). However, larger remains are also present. The maximum length for lithic artifacts is 180 mm of one core on chert from the "Torreón" area and one flake of chert at the test pit zone. Among the osteological remains, we found one fragment of cervid antler measuring 270 mm at the "Torreón" and one rib measuring 260 mm in the test pit area. No major direction of the remains was observed with respect to the archaeological north. Half of the objects showed no inclination (SOM Table S2).

According to the smoothing Kernel density maps, the bone and lithic specimens showed a clustering distribution in the test pit, the central area, and in "Torreón." However, human remains show a restricted dispersion (SOM Fig. S4). L test for inhomogeneous samples shows the following results: the osteological assemblage displays a clustering distribution in accordance with an aggregation model (SOM Fig. S5a). The distribution pattern of the *H. antecessor* specimens indicates a regular dispersion (SOM Fig. S5c). Lithic remains have a regular distribution at distances of less than 80 cm and trend toward clustering at greater distances (SOM Fig. S5b). None of the three groups of objects shows random dispersion. In the "Torreón" area, L test for inhomogeneous distributions suggests a pattern of regular dispersion for the osteological remains at distances less than 20 cm and aggregation of remains at larger distances (SOM Fig. S6). Lithic remains fall within the confidence interval of the Poisson line, suggesting a random distribution of these materials (SOM Fig. S6). Results from the L cross-test support that there is a spatial distribution model of clustering codependence between the osteological and lithic samples of the central zones and the test pit (Fig. 6a) and in the "Torreón" area (Fig. 6b). In the central and test pit zone, there is also a clear spatial association between the remains of fauna and the specimens of *H. antecessor* (Fig. 6c). The spatial model with a tendency to aggregation is also seen between the archaeological remains and clast in central and test pit and "Torreón" zones (SOM Fig. S7, S8).

Table 4 Distribution of bones from TD6.2.4, TD6.2.2/3, TD6.2.0/1, and TD6.1 according the bone structure and shape

	TD6.2.4		TD6.2.2/3		TD6.2.2/3		TD6.1	
	NSP	%	NSP	%	NSP	%	NSP	%
Bone structure								
Cancellous	46	12.8	331	12.7	83	13.5	60	15.0
Cortical	3	83.9	2199	84,2	589	83	332	82.8
Mixed	12	3.3	82	3.1	28	3.5	9	2.2
Shape bone								
Cube	35	10.1	279	10.7	77	10.3	49	12.2
Flat	296	87.4	2257	86.4	599	86.8	334	83.3
Tube	10	2.5	76	2.9	24	2.9	18	4.5

Dense and flat bones (mainly shaft fragments of long bones) characterize the assemblage according to the structure and shape of bones (Table 4, Fig. 4). Seventeen taxonomic groups have been recognized in TD6.2.2/3, including the remains of medium-sized deer and *H. antecessor*, according to the NISP, MNE, and MNI (SOM Table S3). However, the

Simpson index ($D = 0.3426$) and Shannon index ($E = 0.5653$) do not seem to demonstrate a predominance of any species over the others, although a greater presence of artiodactyls and perissodactyls over other taxonomic groups such as carnivores or rodents is evident. The taxonomic composition, besides the presence of cannibalized hominin remains, may be considered the traditional one of the assemblages of anthropic origin during the Pleistocene. Concerning animals, at TD6.2.2/3, a greater presence of adult individuals has been observed. In contrast, another profile age has been identified as *H. antecessor*, since there is greater representation of young individuals. The description is the following: one adult individual of about 17 years old (ATD6-96), one individual between 6- and 10-year-old, another individual 6-year-old, and finally one child who was between 2.5- and 3-year-old at the time of his/her death (Bermúdez de Castro et al. 1997, 2006, 2008; Carbonell et al. 2005; Martinón-Torres et al. 2019). Considering this, we can highlight a greater presence of young in the human sample of this layer, as it seems to suggest the general trend observed along the entire TD6.2 subunit (Saladié et al. 2012).

In TD6.2.2/3, 545 (11.5%) remains show anthropogenic modifications, including faunal and hominin specimens. Almost 40% of upper- and intermediate-limb bones show cut marks (39.2 and 39.6%, respectively). Metapodials have a frequency of cut marks of 20.1%. Among long bones, cut marks are located on the midshafts in 90.5% of the cases. There are also cut marks on elements of the cranial and post-cranial axial skeleton. All these characteristics indicate primary access to the carcasses, without distinctions between different weights of animals and hominin remains. The butchering processes were completed with breakage of the bones, which can be observed in 109 (2.3%) remains. Peeling was documented on 76 specimens. Carnivore's tooth marks were found on 8.5% of the bones, although they have not been recorded on *H. antecessor* specimens. Regarding their distribution, it should be mentioned that 21% of near-epiphysis portions, 16% of epiphyses, and 8.5% of long bone midshafts show carnivore tooth marks. This distribution supports the secondary access of carnivores to the hominin-processed bones of the assemblage, indicating they were modifying agents and not accumulators of the assemblage.

The more abundant postdepositional modifications are the manganese oxide stains that affect 34.7% of the assemblage (SOM Table S4). About 98.2% of them show a dendritic pattern, 0.7% bear mask coatings, and the remaining 0.9% have both types. Regarding the distribution of stains on bone surfaces, most are scattered on all sides of the bones. The next most important postdepositional modification, according to its frequency in the assemblage, is the cemented sediment attached to bones, which is documented in 24.2% of the items. Humidity cracks (3.8%), abrasions (1.8%), trampling (1.2%), and weathering (0.8%) are scarcer. Abrasions affect mostly the edges of the fracture surfaces (68 of 85 specimens). In the rest of the specimens, the abrasion is stronger and can affect the complete fracture surface (0.3% respect to the total of the assemblage); however, the morphology of the bones has not been altered. Weathering has been observed in stage 1 in 78.9 % of the cases (30 of 38 specimens), although seven specimens show stage 2, and one shows stage 4.

Agreeing to the density Kernel maps (Fig. 7a), these modifications do not seem to show a single pattern of aggregation among them in the central and test pit areas, although in some cases we can observe spatial overlaps. Manganese oxide stains, humidity cracks, and abrasion of the edges show some spatial coincidence in the central zone of the excavation according to the visual examination of the density maps. This

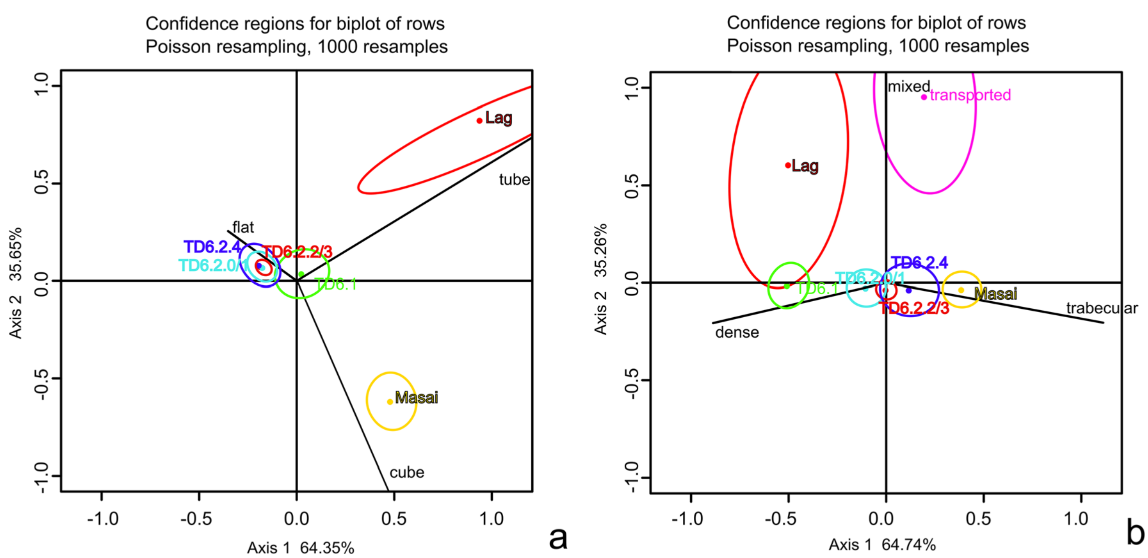

Fig. 4 **a** Simple correspondence analysis displaying the relationships of a lagged, dragged, and home base Masai assemblage, and TD6.1 and TD6.2 layers according the shape of the bones. **b** Simple correspondence analysis displaying the relationships of a lagged, dragged, home base Masai, and TD6.1 and TD6.2 layer assemblages according the structure of the bones

may be related to the zones of circulation of water flows, although the frequency of cracks and abrasions is very low in the whole of the assemblage. In fact, in the same area, there are a greater number of unmodified specimens, so the visual examination of the density maps does not provide a confident observation. If we consider the modifications of mechanical origin that could have been caused by the friction of the sediments, such as the abrasion of the bones and the trampling, the bones with these modifications are not observed to be predominantly in the same place. A multitype cross L function (Fig. 7b) allows us to assume a spatial codependence (in the form of clustering) between the different types of postdepositional modifications in the central zone and test pit of TD6.2.2/3. However, some exceptions can be observed.

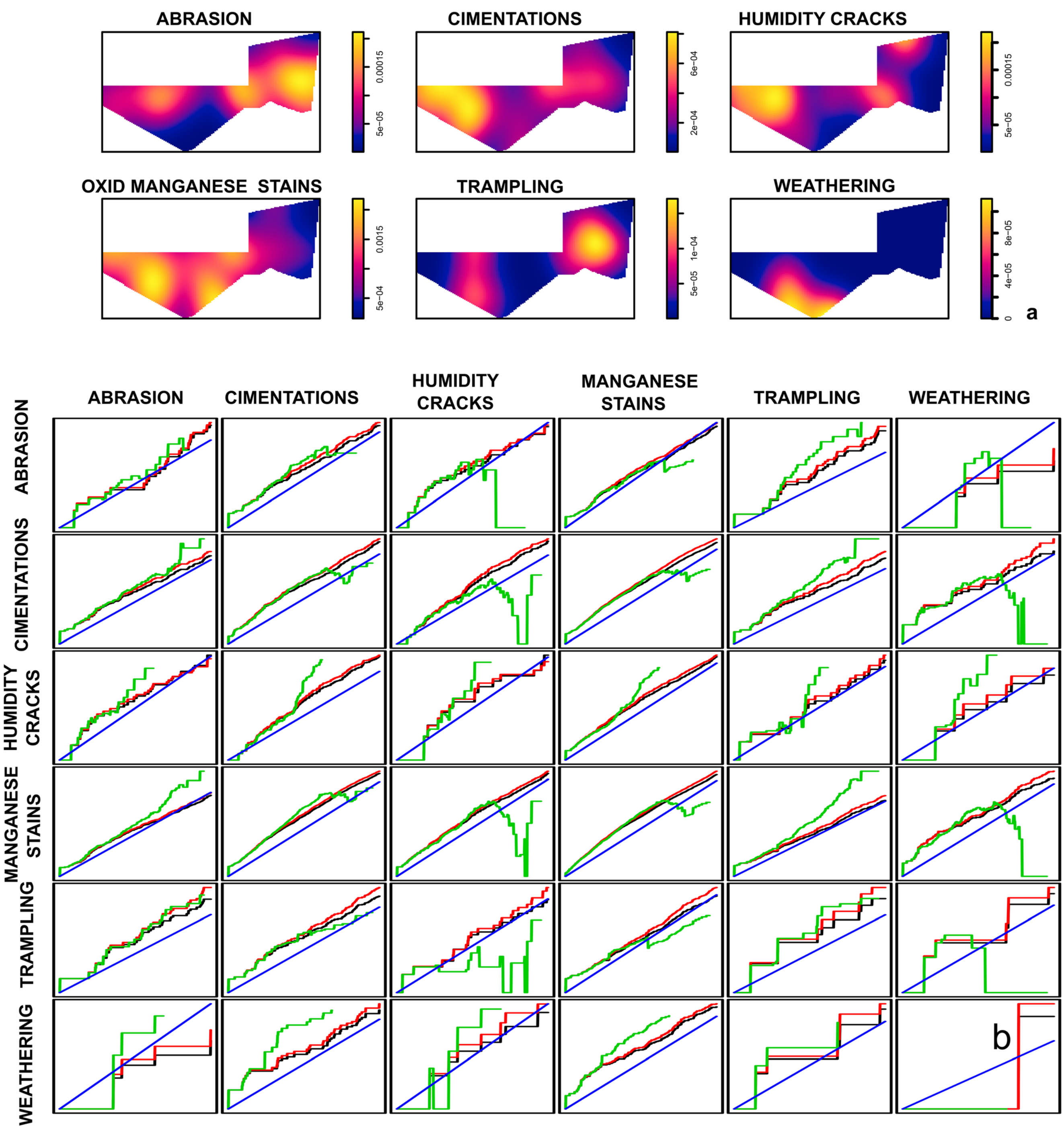

Fig. 5 **a** Kernel density maps of distributions of postdepositional modified and non-modified remains. **b** Multitype L function for osteological remains with postdepositional modifications from TD6.2.4. Ripley's isotropic correction estimate of L (black line): trans, translation corrected estimate of L (red line). **d** Border-corrected estimate of L (green line) compared to the theoretical random Poisson process (blue line)

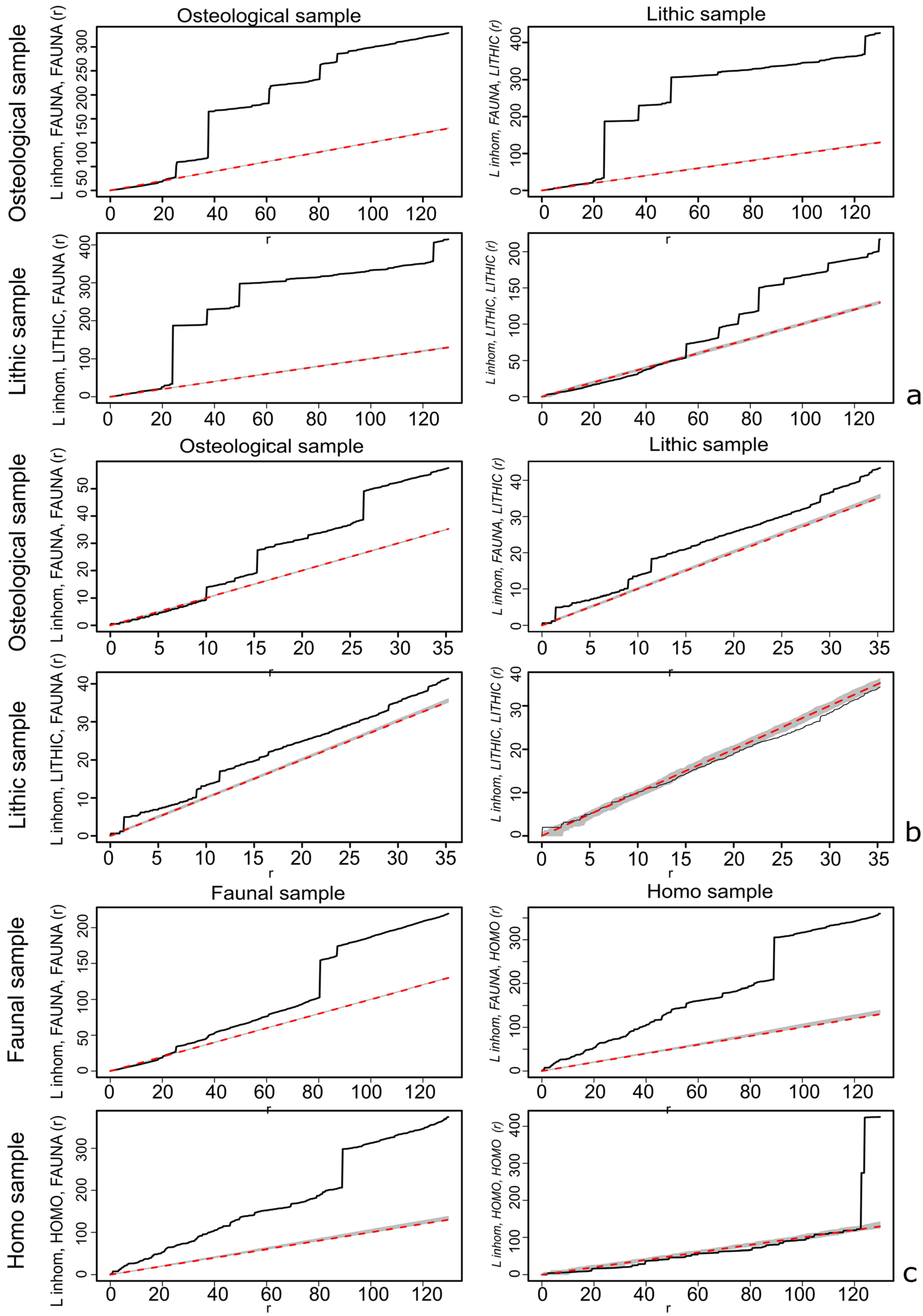

Fig. 6 **a** Multitype inhomogeneous L function for osteological and lithic remains from TD6.2.2/3 in central and test pit areas. **b** Multitype inhomogeneous L function for osteological and lithic remains from TD6.2.2/3 in the "Torreón" area. **c** Multitype inhomogeneous L function for faunal and *Homo antecessor* remains from TD6.2.2/3 in central and test pit areas

Trampling shows a spatial relationship of exclusion with the weathering and the abrasion patterns. There is no spatial relationship between the cemented sediment attached to weathering and between the manganese oxide stains and specimens with trampling. The same dynamics are observed in the "Torreón" area (Fig. 8). The spatial pattern shows a clustering relationship between all postdepositional modifications, except for the specimens with cemented sediment attached and abraded specimens, which do not maintain spatial codependence.

TD6.2.0/1

The TD6.2.0/1 is the top layer of TD6.2 subunit. It is preserved in the central and test pit areas of the excavation surface. Among the inclinations, flat objects (39.3%) stand out

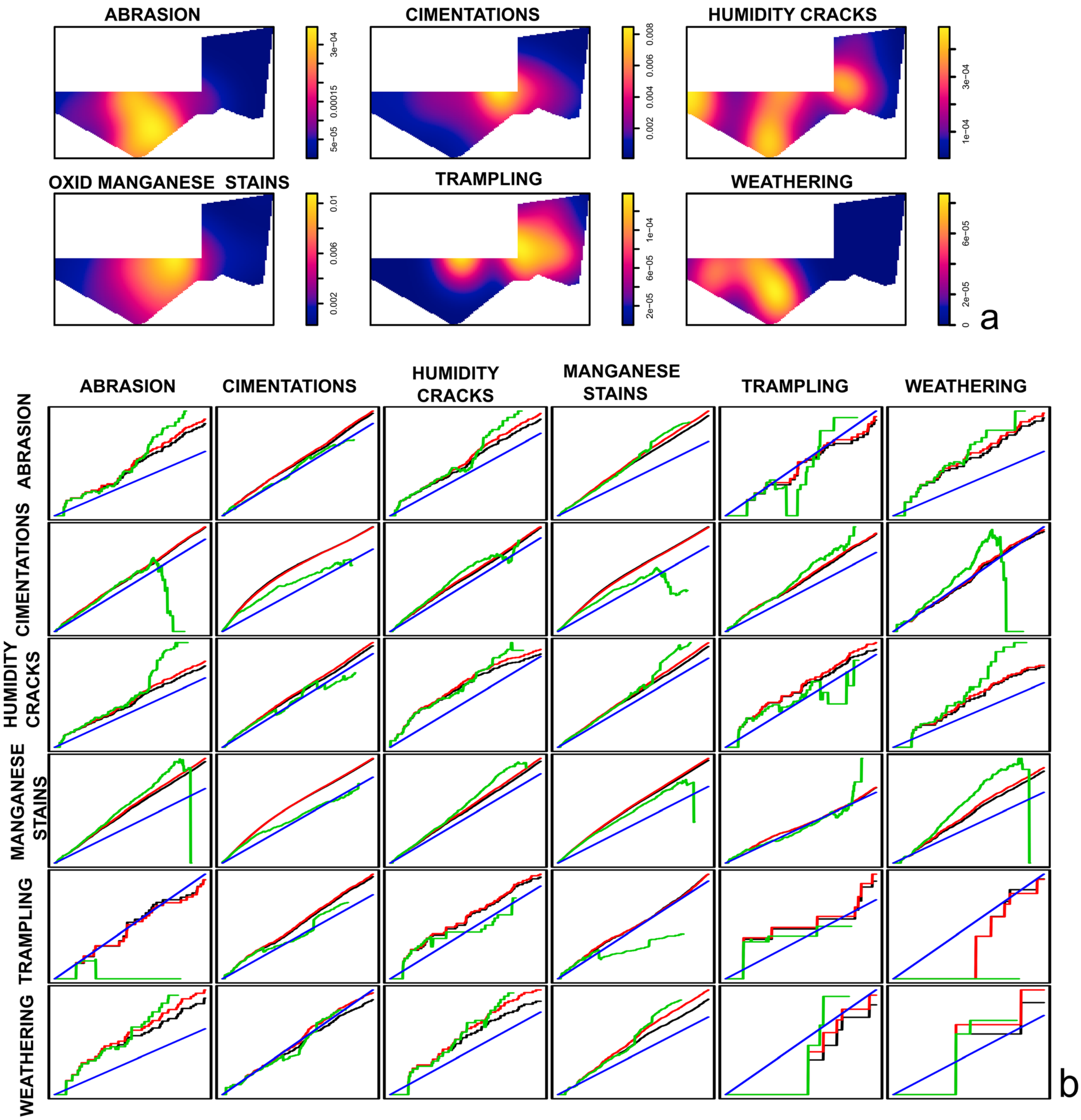

Fig. 7 **a** Kernel density maps of the distribution of postdepositional modified remains from TD6.2.2/3 central and test pit areas. **b** Ripley's isotropic correction estimate of L (black line); trans, translation corrected estimate of L (red line); border-corrected estimate of L (green line) compared to the theoretical random Poisson process (blue line)

(SOM Table S2). A total of 207 lithic tools were recovered. The sample consists of cobbles, fragments of cobbles, hammerstones, cores, flakes, and retouched flakes and contains two groups of refits. The first is made up of one broken flake and one retouched flake, on which the fracture occurred during the process of either detaching or retouching the flake. The second refit is made up of two flakes and one core (Mosquera et al. 2018). The osteological sample is formed by 1086 remains: 62 specimens of *H. antecessor*; 197 faunal remains; and 827 indeterminate fragments (SOM Table S3). Almost half of the remains in both the set of bones and teeth, as in the lithic specimens, are less than 30 mm (48.3 and 49.7%, respectively). However, the other 50% correspond to larger pieces, some exceeding 90 mm (Table 2). A fragment of a diaphysis reaches 200 mm of length, next to a core of Neogene chert that reaches 170 mm of maximum length.

According to the Kernel density maps, the lithic and osteological materials are clustered in the same areas (SOM Fig. S9a, b). L tests (SOM Fig. S9c, d) support a regular dispersion for osteological specimens and random remains for the lithic

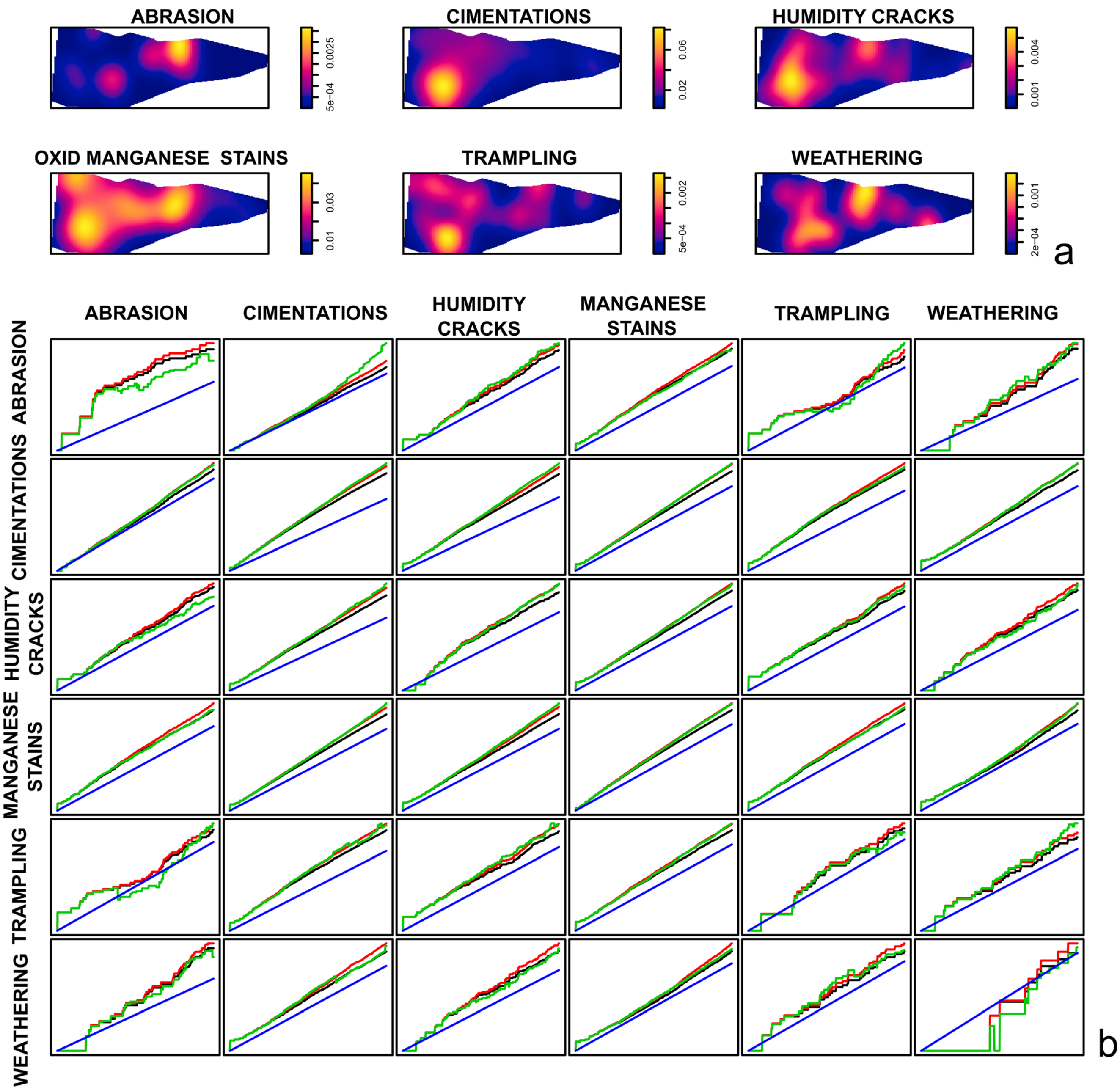

Fig. 8 **a** Kernel density maps of the distribution of postdepositional modified remains from TD6.2.2/3 "Torreón" area. **b** Multitype L function for osteological remains with postdepositional modifications from TD6.2.2/3 "Torreón" area. Ripley's isotropic correction estimate of L (black line): trans, translation corrected estimate of L (red line); border-corrected estimate of L (green line) compared to the theoretical random Poisson process (blue line)

tools. The inhomogeneous multitype cross L function also offers divergent results since it indicates aggregations of bones at distances greater than 100 cm and a model of only slightly of spatial segregation between the lithic remains and the osteological remains (Fig. 9). The same test appoints at an aggregation model in the spatial relation between the archaeological materials and the limestone clast (SOM Fig. S10)

As in the other layers of TD6.2, TD6.2.0/1 is mainly composed of bones with a flat-shape and cortical structure (Table 5, Fig. 4). This is the layer where fewer species have been recognized. At the level of NISP and MNI, medium-sized deer and specimens of *H. antecessor* are the most abundant. Among the specimens of *H. antecessor*, at least seven individuals have been identified: one 17-year-old, two of about 14 years, another between 10 and 11 years, one of 6–9, another of 6 years, and one of approximately 3.5 years when they died (Bermúdez de Castro et al. 1997, 2008). Deer are represented by a MNI of three: one subadult animal and two prime adults. cf. *Bison voigtstendtensis* is represented by two individuals. Other taxa are each represented by one individual per taxon (SOM Table S3). A slight dominance by the two main taxa may be reducing the diversity indices obtained for the assemblage ($D = 0.3426$; $E = 0.5555$), although there is no significant difference as compared to the previous layers.

Cut marks were found on 10.2% of the assemblage. These are found on herbivorous bones, remains of *H. antecessor*, and on one phalange of *Ursus dolinensis* and one cercopithecid phalange. As in the other layers of TD6, cut marks are located on shafts of long limb bones (49.5%) and ribs (12.6%), supporting primary access to fauna and hominins. Anthropogenic bone breakage was observed on 59 specimens, of which 36 show indentations and percussion stigmas. Peeling associated with human specimens was found on 19 items. Carnivore-induced modifications were found on 9.3% (NSP = 101) of the remains. Tooth marks on long bones were found in 50% of the near epiphyses, versus in 21.9% of midshafts and 18.2% of epiphyses. Their disposition matches the secondary access of these taphonomic actors.

Among the postdepositional modifications, the most abundant are those related to humidity and drying periods (SOM Table S4). First, manganese oxide stains are on 32.2% of the assemblage, where 99.2% of the cases show a dendritic pattern, with spots distributed on all surfaces of the bones, including fracture surfaces, articular portions, and muscle insertions. Cemented sediment attached to the bone surfaces can be seen on the 12.3% of the assemblage. Abrasion is present to a slight degree on 63 specimens (5.8%), affecting both the edges of the bone fractures (83.7%) or the entire surface fractures (16.6%). Humidity cracks were found on 4.8% fragments. Weathering and trampling are the lesser postdepositional modifications represented since they are found on 10 remains each. Among the specimens with weathering, four were classified as stage 1 and another four as stage 2. A single specimen for each represents stages 3 and 4. We can see in the Kernel density maps that these modifications are spatially overlapping in the central area of the excavation (Fig. 10a). Cross multitype L function allows us to assume a spatial codependence in all of them, except between weathering- and trampling-modified bones among which there is no spatial relationship (Fig. 10b).

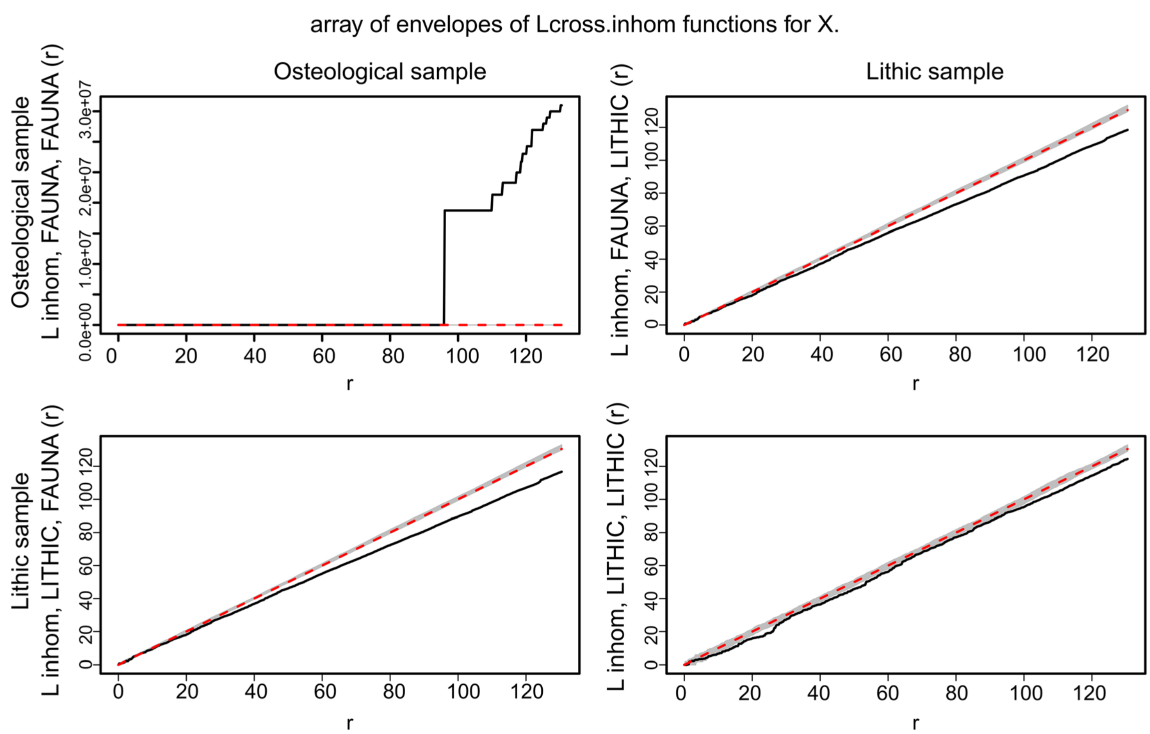

Fig. 9 Multitype inhomogeneous L function for osteological and lithic remains from TD6.2.0/1

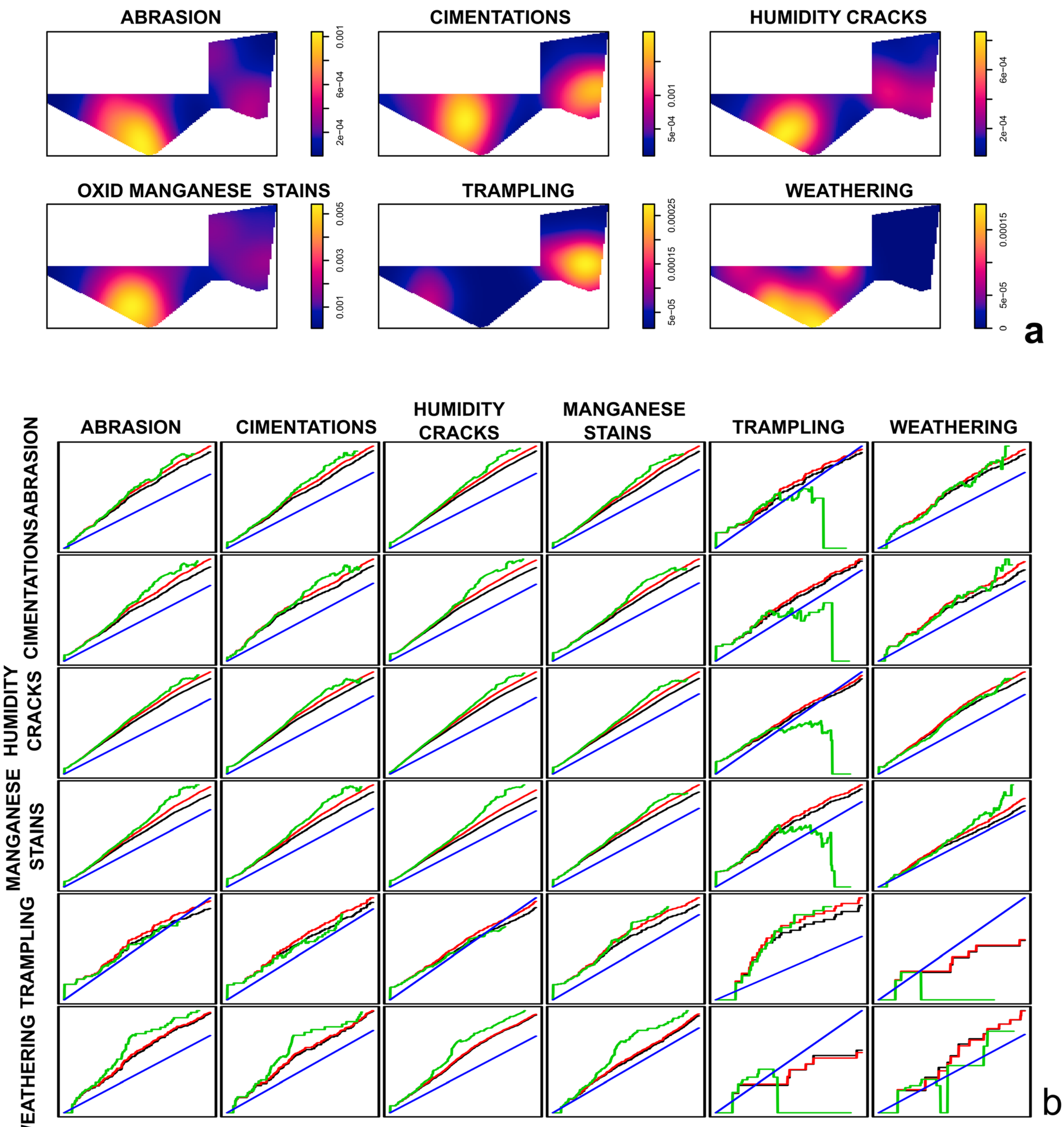

Fig. 10 **a** Kernel density maps of the distribution of postdepositional modified remains from TD6.2.0/1. **b** Multitype L function for osteological remains with postdepositional modifications from TD6.2.0/1. Ripley's isotropic correction estimate of L (black line): trans, translation corrected estimate of L (red line); border-corrected estimate of L (green line) compared to the theoretical random Poisson process (blue line)

TD6.1

The TD6.1 subunit is composed of seven specimens of *H. antecessor*, 112 remains of identified fauna, and 480 taxonomically undetermined bone remains; in total, there are 599 bone and tooth specimens. The objects show a predominant bearing to northeast and northwest respect the archaeological north. The plunges are also diverse, although highlight sunken objects eastward (SOM Table S2). The lithic assemblage is composed by124 items, among which only flakes and retouched flakes are present. This sample does not contain pebbles or cores and also none clear refit has been identified (Mosquera et al. 2018). Around half of the assemblage has a maximum length between

30 and 60 mm. Specimens under 30 mm are also abundant (Table 2). Larger specimens are present, although to a lesser extent. The maximum length of bones is 140 mm (mandible fragment and shaft radius of bison and femur shaft of deer).

Smoothing Kernel density maps show that the osteological and lithic remains are superimposed, although the distribution of lithic remains shows higher dispersion according to visual examination (SOM Fig. S11a, b). The quadrat chi-square test showed that osteological and lithic remains at TD6.1 were distributed significantly differently from a stationary pattern following an inhomogeneous pattern. L tests show a virtual distribution in accordance with a Poisson random pattern both for bones and stone tools (SOM Fig. S11c, d). The multitype cross-inhomogeneous L function suggests a lack of point-type spatial interdependence, since the observed data falls within the confidence acceptance (Fig. 11). A regular spatial distribution is observed between clast and archaeological specimens (SOM Fig S12).

The faunal assemblage is composed of herbivores, among which the medium-sized deer (SOM Table S3) and carnivores stand out. The Shannon index ($E = 0.645$) and Simpson index ($D = 0.3347$) indicate that the set contains certain taxonomic diversity without clear dominance of any taxon. Cut marks were found on 42 (6.9%) remains, among which there is a clavicle of *H. antecessor* and one phalange of *U. dolinensis*. Eight long bone fragments show percussion pits and/or notches on shaft portions. Carnivore tooth marks are on 67 remains. This sample included one phalange of *H. antecessor* with evidence of gastric acid attacks. In fact, this is the only human specimen from TD6 with carnivore modifications. According to the bone shape and structure, TD6.1 comprised mainly flat (83.3%) and cortical bones (82.8%; Table 4, Fig. 4).

The cemented sediment attached to the specimen's surface was found on 32 remains (5.3%) and black stains from manganese oxide deposits affect 18 fragments (3%) (SOM Table S4). These are in the form of detrital stains that affect all the conserved surfaces of the bones. The disposition pattern on the surface of the bones is dispersed in all cases, without distinctions between the articulation and insertions and the rest of the areas of the bones. Mechanical modifications as abrasion and trampling are on 2.6 and 0.5%, respectively. Cracks produced by weathering (stage 1) were documented on 2.4% of the sample. All changes were in the same area, showing spatial overlap. Their low frequency does not seem to agree with large movements of the remains. However, the small sample size does not allow for reliable estimates. Abrasion shows spatial codependence in the form of clustering with weathering, trampling, attached cemented sediment attached, and manganese oxide stains. The same relationship is observed between attached cemented sediment attached with manganese oxide stains and trampling. The other combinations show no spatial relationship (Fig. 12).

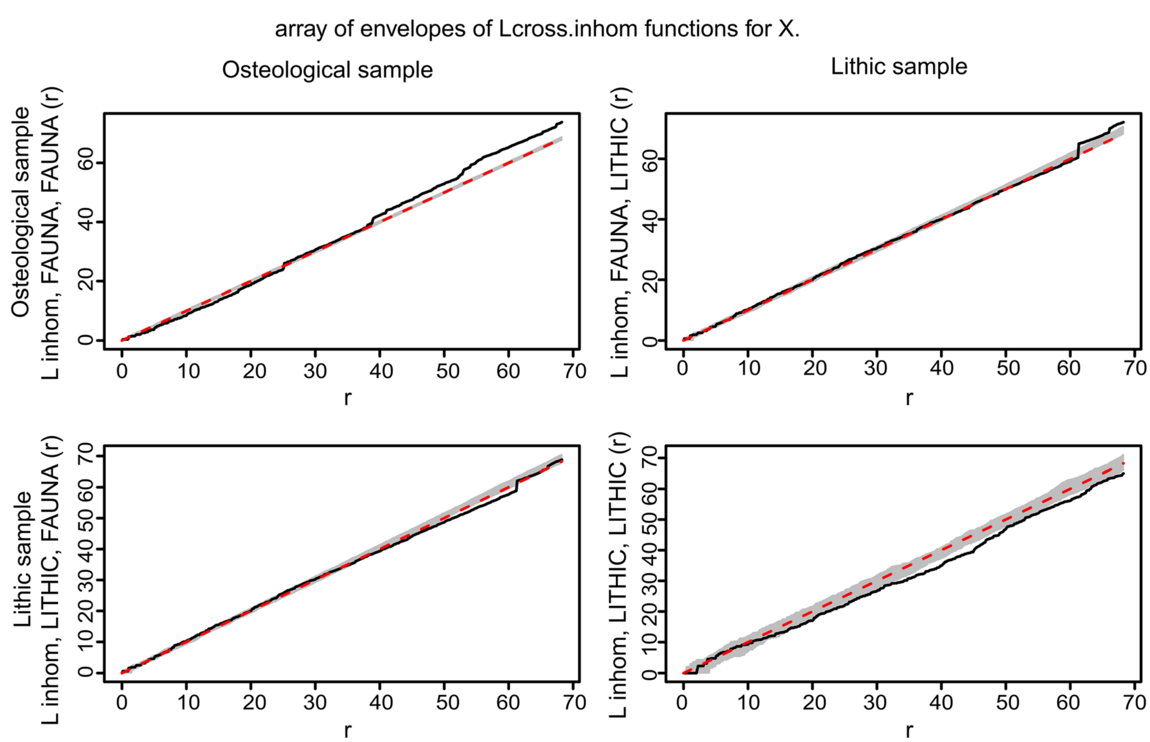

Fig. 11 Multitype inhomogeneous L function for osteological and lithic remains from TD6.1

Vertical distribution

The vertical distribution of lithics and osteological sets fromTD6.1 and TD6.2 subunits is globally bimodal and almost symmetrical (Fig. 13). At the bottom of the sequence—distribution corresponding to TD6.2.4—an abnormal value is observed in the line corresponding to the osteological remains. However, the distribution of the lithic items resembles that of the fauna except at this point. The distribution of both lines can be influenced by the higher density of remains in the TD6.2.2/3 layer. In the vertical distribution of the clasts, we can observe differences with this model. The distribution of clasts is left-skewed and follows a multimodal pattern with greater weight at the bottom of the sequence, coinciding with TD6.2.4 level. However, lower weight was detected in the presence of blocks coinciding with the area where there is a higher density of archaeological materials.

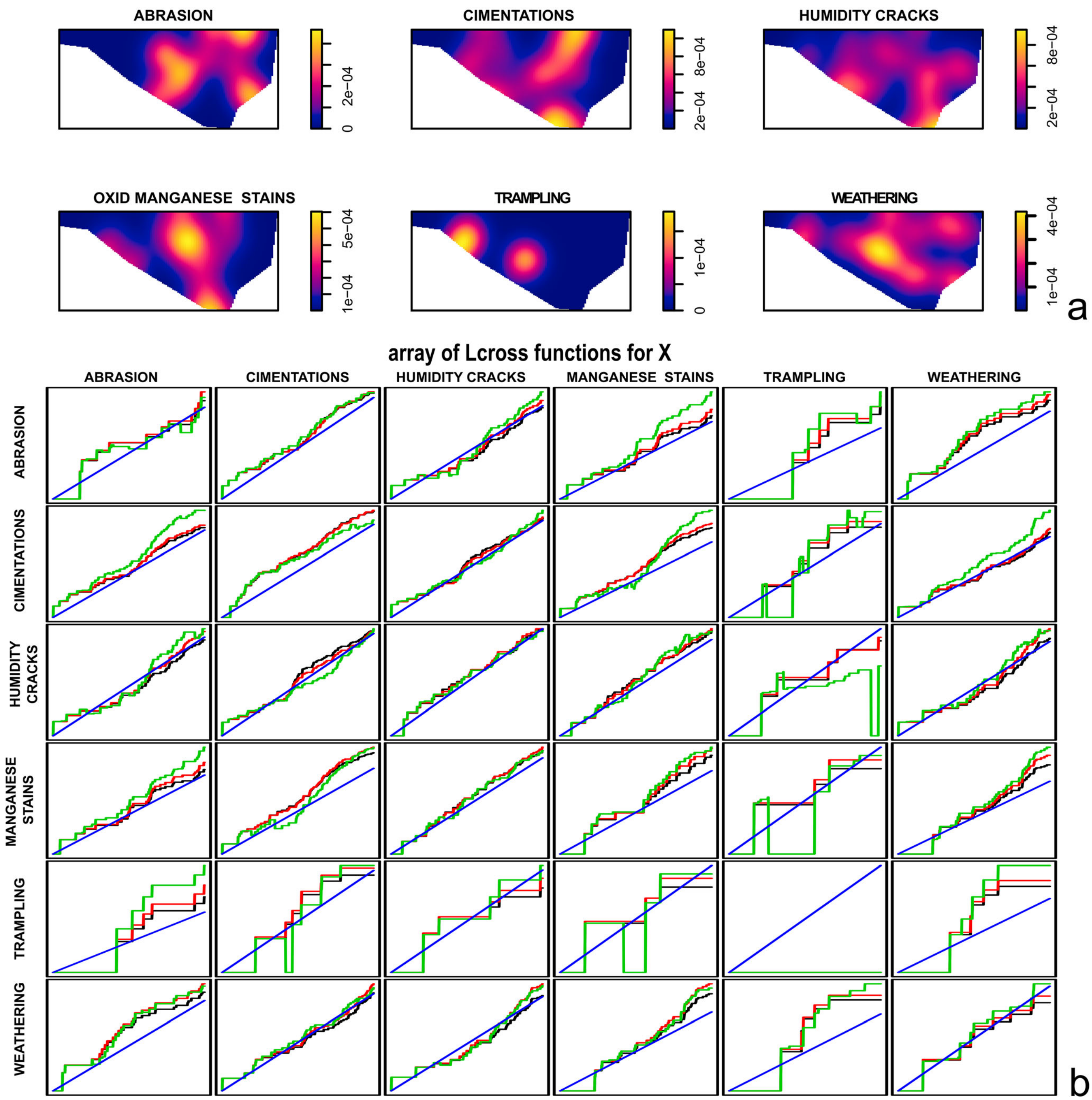

Fig. 12 **a** Kernel density maps of the distribution of postdepositional modified and non-modified remains. **b** Multitype L function for osteological remains with postdepositional modifications from TD6.1. Ripley's isotropic correction estimate of L (black line): trans, translation corrected estimate of L (red line); border-corrected estimate of L (green line) compared to the theoretical random Poisson process (blue line)

Discussion

The excavation of the sediments with anthropogenic materials of TD6 in the scarce 6 m^2 of the test pit turned out to be a key discovery for our knowledge of the first human prehistoric settlement in Europe. As a result of the study of the sediments excavated and the materials recovered, new chronologies of occupation of the continent and the Iberian Peninsula were proposed (Parés and Pérez-González 1999); a new hominin species was described (Bermúdez de Castro et al. 1997); the oldest incidence of the unusual behavior of cannibalism perpetrated by our genus was documented (Fernández-Jalvo et al. 1996); and the possibility of new debates has arisen regarding dispersals and the ecological and economic aspects of these past populations of the Iberian Peninsula (Carbonell et al. 1999b). According to the complete study of the sample, Bermúdez de Castro et al. (1999: 696–697) described the TD6 unit as "… a space that was frequently used for several activities, some of which were carried out from beginning to end in the cave." Since then, research on the assemblage has been refined, in accordance with the enlargement of the surface of excavation as well, increasing the volume of remains to study in turn. The extension of the excavated surface resulted in a more complex stratigraphy in which strong lateral variations between the two ends of the section and the central zones were identified, as well as a succession of different sedimentary facies. Campaña et al. (2016) described up to nine sedimentary facies in the sequence of this new sedimentological panel of TD6.2 and TD6.1. According to their observations, the different layers are made of a mixture of channel facies, debris flow, food plain, and decantation. The origin of archaeological materials agreeing to this model is, at least most of them, allochthonous and they, therefore, proposed that the remains of human activity once deposited behaved as clasts and bioclasts inside the sediment of cave infilling. If this model was correct, the fossils of TD6.2 and TD6.1 would come from outside the cave and be deposited in the cave entrance area by different geological processes (gravity flows and fluvial flows) and likely in different time lapses.

This would doubtless raise questions about some previous studies' conclusions, especially the interpretation of the assemblage as the product of the activity of the hominins in a home base (Bermúdez de Castro et al. 1999; Carbonell et al. 1999b; Saladié et al. 2011). However, we argue that the sedimentary processes are not continuous over time (Arche 1989) and may need a large amount of time for the formation of the deposits (Luckman 2013), which could lead to independence between the accumulation of the sedimentary particles and archaeological remains. Campaña et al. (2016) observed weathering processes in clasts along some of the layers described in TD6.2.0/1 and TD6.2.2/3. This has important implications regarding the existence of possible temporary hiatuses, without erosion or sedimentation, during which hominin activity could have developed in the first place and subsequently followed by carnivore activity. This sequencing was already observed in the taphonomic studies conducted by Saladié et al. (2011, 2014).

An important problem is that today, there are not available actualistic frameworks about the composition of the fauna groups produced by a debris flow. Besides, most studies from a taphonomic perspective are of assemblages from prehistoric periods before the genus *Homo* emergence (e.g., Britt et al. 2009; Domingo et al. 2017). However, it has been found that the gravitationally accumulated sets are challenging to infer through the taphonomic models obtained since these carry-overs do not significantly influence their composition (Britt et al. 2009). This characteristic fact makes it difficult to establish robust analogies with the TD6 assemblages where humans, as actors, and tools, as effectors, come into play, affecting the taphonomic history whether or not the aforementioned transport and its reworking exist.

If the debris flow has no effect on the classification by size or shape of the skeletal elements, we can assume that this will be similar to the lithic tools. However, water flows can alter the composition of the original set (Boaz and Behrensmeyer 1976; Petraglia and Potts 1994; Aslan and Behrensmeyer 1996). This difference should be observed in the distribution of the subunit TD6.2.2/3 since it is where there is a greater diversity of facies. In this sense, according to Campaña et al. (2016), there are lateral sedimentary changes of debris flow facies, channel facies, and floodplain facies. However, the assemblage homogeneity does not allow observing the differences between the different types of sedimentary processes on the osteological sample. It is significant, no differences were observed in the spatial distribution of the postdepositional modifications, and not exist dissociation of the archaeological remains of the subunit.

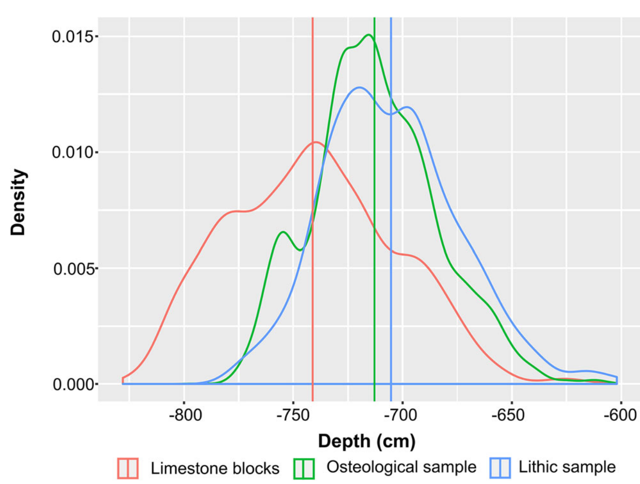

Fig. 13 Vertical distribution of lithics and osteological remains from TD6.1 and TD6.2 subunits

We have more tools to evaluate the effect of the water currents that could affect the remains deposited in the central area and the test pit throughout the entire unit. According to the current observations, water flows tend to disperse previously accumulated objects at any place, reducing the number of remains of the original set (Schick 1987; Rogers and Kidwell 2007). Therefore, in lag assemblages, it is common to have disturbances in original materials' associations and composition (Schick 1987). Recent research on the lithic technology of Unit TD6 indicates the existence of 12 groups of refits comprising 26 pieces in the three archaeological sublayers of TD6.2 (Mosquera et al. 2018). However, while water currents can be expected to reduce the number of traceable pieces (Petraglia and Potts 1994), it has also been shown experimentally that after water disturbance, some groups of refits may remain in the lag assemblage. Even so, we find in TD6.2 several pieces of evidence that call into question the allochthonous origin of at least these pieces. First, refits are usually retained in the lag assemblages but less frequently in the dragged ones. Second, when refits are retained, they tend to be separated from each other by several meters (Schick 1987). In TD6.2, only one refit was found at several meters. The rest are close refits found at distances of less than 1 m, with some of the cases being knapping accidents.

On the other hand, the refit at a greater distance belongs to layer TD6.2.2/3 and is composed of three parts, a core and two flakes. It is a refit of the knapping sequence, meaning that the distance between pieces seems to respond to their knapping, transport, and likely use (Mosquera et al. 2018). The number of refits may indeed seem low. However, Neogene chert's most common raw material is usually poorly preserved in the Atapuerca deposits, which poses substantial limitations to the refitting studies. Finally, some of the refitted items were assigned to different facies by Campaña et al. (2016). For example, we find a refit that join remains coming from food plain and debris flow facies (1995 TD6.2.2/3 H17 n° 137 + 2003 TD6.2.2/3 G11 n° 1 + 2007 TD6.2.2/3 F12 n° 147) and another whose pieces are found in the channel and debris flow facies (2007 TD6.2.2/3 E13 n° 130 + 2007 TD6.2.2/3 F13 n° 395), respectively (Campaña et al. 2016 fig. 3; Mosquera et al. 2018 fig. 26), which calls into question their interpretation of the depositional independence of the archaeological materials in each of the facies.

The spatial disturbance of objects and composition of the assemblages transported en masse and affected by water flows can be evaluated through different parameters, both lagged and dragged assemblages. According to the reference frameworks available, water transport can select the remains according to their size (Shipman 1981; Schick 1984; Pante and Blumenschine 2010). Small debris remains or fragments of bones smaller than 20 mm are particularly vulnerable to fluvial winnowing and subtraction from the original deposition site (Schick 1984; Schick 1987; Pante and Blumenschine 2010). However, under high-energy current conditions and mass transport, cores and large tools could also be long-distance transported (Schick 1984; Schick 1987; Petraglia and Nash 1987). Besides, the greater or lesser presence of small elements is also determined by the degree of bone breakage and the presence of stone tool knapping in the original assemblage (Domínguez-Rodrigo et al. 2014). In the different archaeological layers presented in this study, no metric bias is observed in any category, although it should be noted that in TD6.1 bones of less than 30 mm are less abundant than in the lower layers. Larger bones (>90 mm) are scarce in all layers. Although this could be interpreted as the product of the selection by the influence of water currents, we can reject this hypothesis considering that it is common for bones of larger dimensions to be infrequent in assemblages in which hominins and carnivores have participated in fracturing them (Bunn 1983), as in the case of TD6.2 and TD6.1 (Saladié 2009; Saladié et al. 2011, 2014). Among the stone tools, the metric behavior of the pieces is similar. In fact, there are abundant flakes, fragments of flakes, and knapping remains at all layers, except in TD6.1. The smallest pieces are found next to cobbles, fragments of cobbles, and cores. This is in addition to the presence of short-distance refits, already mentioned above, as well as the presence of the entire production process of the lithic tools in subunit TD6.2 (Mosquera et al. 2018), which seems to agree with the fact that it is a set that is not very disturbed. Unfortunately, the study in degrees of the orientation of the objects cannot be treated since it is not usually recorded in the Gran Dolina excavation, and we cannot do a deep analysis of the fabric. However, the high percentage of objects with a plunge angle of 0° (or near to 0) agrees with strongly undisturbed sets by debris flow. More debatable is the case of TD6.1. However, we are aware that we must exercise caution with these data concerning the method of recording the orientation.

The presence of anthropogenic bone breakage and the evidence lithic tools' knapping is typical of the debris abandoned in the contemporaneous living floor. These debris usually show spatial models that reflect specific socioeconomic behaviors through the spatial interdependence between tools and bones (Domínguez-Rodrigo and Cobo-Sánchez 2017). High fluvial energy currents can modify the associations between both types of materials—modification that should be visible in the lagged and dragged assemblages, again. In the case of some talus deposits formed by rock debris streams (debris flow), the destruction of fossil assemblages has also been argued (Tanner and Hubert 1991). According to the taphonomic interpretations, the record of TD6.2 was accumulated by repeated occupations in which activities such as the transport of carcasses and butchery and consumption of the meat and marrow were developed (Saladié et al. 2012, 2014). It must also be noted that there was transport of raw material, knapping, and use of tools (Carbonell et al. 1999b; Mosquera et al.

2018). If these activities took place in the space in which the archaeological materials have been recovered, it is to be expected that we would find spatial distribution models that show codependence, despite the scarce excavated surface. L and L cross tests indicate that there are different spatial distribution patterns in the different layers. On the one hand, these tests indicate that the osteological and lithic samples' spatial distribution from TD6.2.4 and TD6.1 is random. This differs from TD6.2.2/3 and TD6.2.0/1, where there is spatial dependence with tendencies toward aggregation in the first case and with regular distribution in the second. On the other hand, when we evaluate the codependence between the osteological sample and the lithic sample, patterns of aggregation between both types of materials are observed in TD6.2.4 and TD6.2.2/3 (Figs. 3 and 6); a slight spatial codependence of regular type in TD6.2.0/1 (Fig. 9); and a random association in TD6.1 (Fig.11) (Table 5). Thus, TD6.1 is the only subunit that does not demonstrate any spatial dependence or aggregation between the materials deposited.

According to these results, the horizontal and vertical spatial association between the types of remains can be considered spatially codependent and statistically confirmed in the three sublayers of TD6.2 (Fig. 13). Considering the horizontal data, TD6.1 seems to show a random association. The association between clasts and archaeological remains shows different characteristics. Horizontal codependency is demonstrated in all layers except TD6.2.4. However, the vertical distribution demonstrates clear independence between natural rocks and archaeological materials, pointing out that there is no association in each other's accumulation events. The vertical distribution of the lithic and bone remains does not seem affected by strong gravitational effects since they show an almost normal distribution. Their almost identical distribution would be supporting that it is not the fruit of reworked assemblages.

Other evidence spatial statistics tests the spatial statistics that allows us to evaluate if the assemblages are more or less disturbed. According to the experiments with high and low energy flows conducted by Domínguez-Rodrigo et al. (2018), the segregation of materials is mainly related to the shape of the bone and the tissue type. In TD6.2 and TD6.1, there is a strong predominance of bones of flat morphology and cortical tissue, mainly represented by diaphyses of long bones. To evaluate the composition of the layers identified in TD6.1 and TD6.2, we performed three correspondence analyses considering the shape and structure of the bones from the four archaeological layers, from one sample of an undisturbed Masai Camp, one sample corresponding to a lag association, and one experimental sample of periautochthonous drag (with a maximum transport distance of 20 m; Domínguez-Rodrigo and Cobo-Sánchez 2017; Domínguez-Rodrigo et al. 2018, 2019a). Figure 4a represents a simple correspondence analysis where the four archaeological assemblages are homogeneous, showing a similar representation of bones according to their shape. The graphic representation statistically supports the greater presence of flat-shape bones and the greater absence of cubes and tube-shaped fragments. In this analysis, TD6.2.4, TD6.2.2/3, TD6.2.0/1, and TD6.1 are situated at a Euclidean distance like the lag model and the model of the undisturbed Masai Camp. The result of the transported set is located outside the graph, which indicates that the entirety of unit TD6 could be formed by in locus deposited remains and may be lagged by taphonomic processes that modified their composition. The result of the analysis of simple correspondences according to the bones' structure (Fig. 4b) from the layers of TD6.2 offers a result very close to that obtained by the group from the undisturbed campsite. TD6.1 shows a similar distance between a lag and campsite models. Finally, in the multiple correspondence analysis (Fig. 14), the four layers are grouped in the same area, located near an undisturbed sample. However, TD6.1 is closer to the lag model, which supports a greater loss of less dense materials in this set than in the others. The three correspondence analyses seem to be consistent with the same result. All layers seem to be slightly disturbed, but far from the transported sample. Currently, the referential frameworks that we have are still limited, so these inferences, although solid, should continue to be investigated in the future.

If we consider that the covariance and codependency between materials have not been lost either horizontally or vertically in the layers of TD6.2, it follows that the deposition of the remains was in locus and they do not have a transport origin. Although there is a slight loss of materials, whose structure is mainly spongy tissue, the spatial dependence has survived, so the processes, although disturbing the osteological sample, have not segregated between fauna and industry.

Table 5 Synthesis of the spatial relation of the osteological and lithic remains from TD61 and TD6.2 subunits

	Clark-Evans test	Osteological sample	Lithic tools	Relation faunal-lithic remains
TD6.2.4	Clustering	Random in short distances	Random in short distances	Overlapping/codependence
TD6.2.2/3	Clustering	Spatial dependence, aggregation	Spatial dependence, regular dispersion and aggregation in long distances (more than 80 cm)	Overlapping/codependence
TD6.2.0/1	Clustering	Spatial dependence, regular dispersion	Spatial dependence, regular dispersion	Overlapping/codependence
TD6.1	Clustering	Random	Random	Random

In this regard, it is well known that most processes and taphonomic agents affect the bones according to their density, as they are more susceptible to disappearing than samples mainly formed by spongy tissue. Four factors point to the looting by carnivores of meat residues and other tissues abandoned by hominins (Saladié et al. 2014). These factors are (1) the distribution of cut marks on the skeleton and their frequencies, and percussions mainly made in the central areas of the diaphysis of the long bones of the upper and intermediate elements of the extremities; (2) the frequency of near-epiphysis portions, flat, and compact bones with carnivore tooth marks; (3) the disappearance of most elements of the axial skeleton; and (4) the low presence of epiphyses of long bones (ratio epiphysis/diaphysis = 0.05). If we also consider the presence of small remains, both osteological and lithic, we can rule out that physical transport processes may have caused this reduction. TD6.1 shows a similar model to TD6.2 regarding the internal composition of the bones according to their shape and structure. However, unlike the other assemblages, there is no dependence between osteological and lithic samples. This loss of spatial association suggests that removing of materials could be the product of postdepositional processes that altered previous associations. In this case, the perturbation by water currents seems to be the most parsimonious hypothesis, considering the absence of flakes and knapping waste, the absence of refits, and the remains' size. However, there are two issues to be clarified: (1) the observed pattern of TD6.1 indicates that it is a set also deposited in locus, very far from what matches with a dragged set; and (2) taking into account

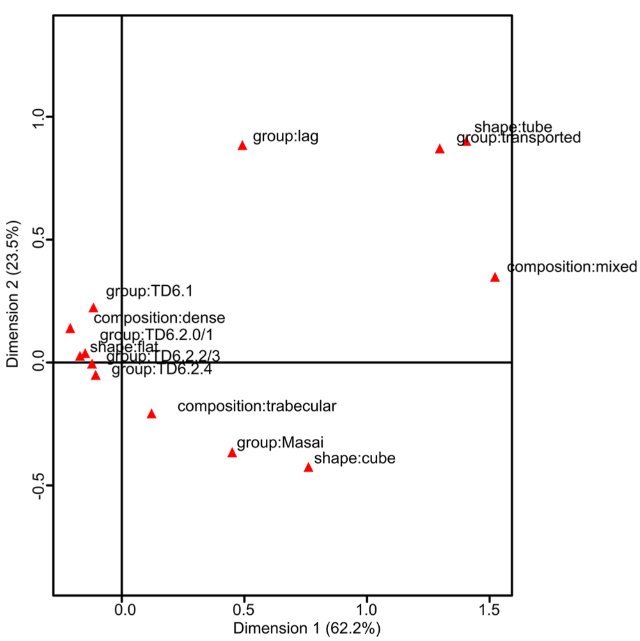

Fig. 14 Multiple correspondence analysis displaying the relationships of taphonomic variables according to bone shape and structure and their relationship with a lagged, dragged, home base Masai, and TD6.1 and TD6.2 assemblages

the composition of the assemblages of fauna and *H. antecessor* specimens, the first origin of the deposition of these remains is the same or similar to that observed in the layers of TD6.2, with hominins being the principal actors. TD6.1 lateral changes regarding the increase of coprolites and a decrease of anthropogenic activity could be the consequence of erosions related to water flow processes.

The postpositional modifications of the assemblages do not contradict these interpretations. Campaña et al. (2016) relied on the frequencies of the postdepositional modifications described in Saladié et al. (2011) to defend their hypothesis on the secondary position by transporting of the fauna and *H. antecessor* specimens inside the sediments. For Campaña et al. (2016), weathering fits with the origin of the archaeological specimens from outside the cave. Behrensmeyer (1978: 153) defined weathering "as the process by which the original microscopic organic and inorganic components of bone are separated from each other and destroyed by physical and chemical agents operating on the bone in situ, either on the surface or within the soil zone." Weathering is the damage to bones produced by exposure to the elements and atmospheric changes before their burial. Bones and teeth are heated and cooled, moistened and dried, and frozen and thawed. These processes may produce a range of changes, from slight modifications (cracks and slight flaking) to complete destruction the bones when they are not protected by the sediments. In TD6, weathering is one of the less abundant modifications, and in most cases, it is found in stage 1 of the stages proposed by Behrensmeyer (1978). However, although weathering severity may be directly related to the time of bone exposure, weathering proceeds at different speeds in different microenvironments (Gifford 1977; Behrensmeyer 1978), which makes it difficult to establish standard ratios. The low frequency of fissures due to subaerial exposures and their low incidence in the TD6 fossils may be related to the fact that weathering, in general, is usually lighter when the bones are protected by vegetation or when they are in caves (Shipman 1981), and certainly not when the bones are located in the open air, where they are exposed to sun radiation.

It seems that Campaña et al. (2016) assumed that changes in temperature, humidity, or freezing only affect the bones in open and uncovered spaces. The sediments excavated in TD6 belong to the cave entrance area, and not to the interior and dark areas, where the microenvironment undoubtedly has greater stability, so these and other modifications are usually less important. If we were in the cave's interior and dark zones, it could be tentatively presumed that we would not find the remains in locus of an anthropic occupation since the microenvironment itself would make the occupation difficult.

The presence of bones with abrasion could support at least one entry of a small portion of material from another point of origin. This modification exists in all layers, being found in less than 2.5% of the remains, except in TD6.2.0/1, which affects 5.8% of the remains. Shipman (1981) attributed the rolling of the edges to sediments transported by water, although there may be no correlation between the distance of transport and the degree of abrasion of the bones (Aslan and Behrensmeyer 1996), since abrasion can be produced by particles transported by air and water (Bromage 1984) with no need for the specimens to be transported. The little movement of the remains would also explain the scarce presence of trampling in the bones of TD6 since this modification is expected to be more abundant if the remains were transported. Short displacements can leave little evidence on bone surfaces, being the segregation according to its structure and forms the most reliable evidence we currently have (Domínguez-Rodrigo et al. 2019a). The microwear analysis conducted on the test pit lithic assemblage for functional purposes showed relatively good preservation of the stone surfaces (Sala 1997; Carbonell et al. 1999b; Márquez et al. 2001). Excluding the macroscopically evident strong alteration of the chert, especially the Neogene variety, as well as the loss of grain cohesion suffered by the sandstone specimens, the pieces made of quartz and quartzite revealed good microscopic surface preservation. Although light to mid postdepositional surface modifications (PDSM) have been reported, strong erosion or edge abrasion pointing to transported pieces was not recorded in any case. As in the Middle Pleistocene TD10.1 subunit of the same site (Pedergnana and Ollé, in press), these PDSMs were interpreted as slight abrasion deriving from the presence of abrasive particles being transported by water, from the pressure of the sediments, and/or just by very short displacements. These PDSMs sometimes limited but did not prevent the traceological study.

The most abundant modifications of the assemblages were not produced during a possible transport. The uniformity in the distribution of manganese oxide stains, their location at the edges of fractures in fresh and dry fracture edges of the bones, and the absence of secondary coatings and masks suggest that they were formed once the bones were buried under conditions of sedimentary water saturation (López-González et al. 2006). Postdepositional modifications related to wetting and drying processes, such as sediment cementations and humidity cracks, show spatial distributions of aggregation between them and with manganese oxides at all layers. This would be in accordance with the presence of small runoffs or puddles in fluctuating drying periods, as sedimentological observations also suggest.

If we consider all the evidence, the archaeological groups that form TD6.2 preserve high integrity and resolution for their archaeological interpretation. According to the composition of abundant bone remains with taphonomic modifications, we can interpret (1) that hominins transported carcasses or parts of carcasses inside of the cave; (2) that they intensively fractured and discarded the bones, in search of the marrow; and (3) in a place where they also introduced lithic raw materials of different varieties, they knapped them and used the lithic tools. Besides, the recent analysis of the anisotropy of magnetic susceptibility distributions in the lower part of TD6.2 shows evidence for and a very low-energy hydrodynamic sedimentation regime (Parés et al. 2020). No signs of fabric disruption or evidence for massive transport of the sedimentary particles (Parés et al. 2020) had been observed, concluding that there had been no postdepositional perturbation in the TD6 unit. These conclusions allow us to defend our inferences with greater force.

In the different studies in which these activities have been described (Carbonell et al. 1999b; Díez et al. 1999; Saladié et al. 2011, 2014; Mosquera et al. 2018), the TD6.2 subunit has been reported as the fruit of the hominin activity at a home base. According to Isaac's (1978) definition for home base, which he redefined as a central place of foraging (Isaac 1983), it is a place where the resources obtained are shared and the center of the social activity for groups of hunter-gatherers. In these settlement models, bones and stone tools usually remain grouped in the same places. The concentrations of bones are the residues of hunting, transportation of carcasses, food-eating, and the possible ravaging by carnivores (Stanford and Bunn 2001). The lithic raw material is also transported and perhaps accumulated, and the lithic tools are elaborated, used, and discarded. The presence of large cores of Neogene chert, showing different stages of production and removals of several pieces in their surfaces, indicates sequences of knapping in place and reinforces the idea of structured occupations according to a clear plan (Carbonell et al. 1999b; Mosquera et al. 2018). Other daily and social activities, such as meat sharing, probably took place in the same area, although we do not have archaeological evidence for this.

So far, TD6.2 is the oldest European assemblage with these characteristics. It is to be expected that soon, more evidence will appear with similar characteristics in nearby geographical areas, as penecontemporaneous or even older deposits are more and more abundant (e.g., Arzarello et al. 2007; Bermúdez de Castro et al. 2008; Toro-Moyano et al. 2013; Vallverdú et al. 2014). Indeed, to date, TD6.2 is the only site that preserves high integrity and excellent preservation of the remains that allows us to investigate the behavior of the first European populations through the abandoned remains in a well-preserved living floor. This is especially important to keep in mind since most TD6 sediments will be excavated in the future.

Conclusions

The present evaluation of the TD6.2 hominin-bearing deposits at Gran Dolina indicates that the archaeological specimens were preserved in locus since nothing indicates reworking, outside origin and subsequent transport inside the cave of the archaeological remains. The archaeological materials from the TD6.2 layers show spatial codependence between stone tools and osteological remains, structural properties impossible to maintain in assemblages transported in same meters, neither by high energy flows nor by low energy flows or gravitational action. Other pieces of evidence supporting the deposition in locus are the presence of elements of all sizes and the short-distance lithic refits, some of them related to knapping events. All available evidence supports the idea that the archaeological materials of these layers are the product of anthropogenic activity in a place of residential activity. Although carnivores are the main cause of the loss of osteological material, the sequence observed in TD6.2 suggests that carnivores' ravaging after hominin activities did not disturb the initial spatial associations, at least considerably. However, their activity is observed in the removal of cancellous tissue portions (postcranial axial skeleton and epiphyses). The composition of the materials according to their shape also was altered, hence the overrepresentation of flat bones mainly represented by diaphysis of long bones. This character is also the result of the loss of elements of lower density (cancellous and mixed structure).

Regarding TD6.1, despite showing the same pattern in the structural features of bones, the spatial associations are random. This highlights the independence between stone tools and osteological materials. In this group, a reduced presence of smaller materials and the absence of lithic refits have also been reported. These characters suggest that, despite possible ravaging of carnivores, other processes also affected the assemblage, perhaps water flows. However, the assemblage does not correspond to a dragged assemblage, but to a lagged one. Consequently, the archaeological material of TD6.1 was deposited in locus by the hominins, in the same way as TD6.2, at least in the space in which the sample has been preserved.

The four assemblages studied (TD6.2.4, TD6.2.2/3, TD6.2.0/1, and TD6.1) show a similar composition of structural characters of the bones. This is not surprising if we consider that most of taphonomic actors and processes modified the composition of archaeological samples in correlation with the density of bones and their portions. The proxies used by the methodological approaches related to spatial taphonomy have been key tools in evaluating the alterations that affected these assemblages by postdepositional processes.

Layers of TD6.2 have the highest integrity and expected preservation in an Early Pleistocene assemblage, considering that during the formation of the deposits, the processes of accumulation and reduction are common in a systemic context, and neither the sedimentary processes nor the anthropogenic activity is continuous overtime in the studied deposits. Reaffirming our previous interpretations (Saladié et al. 2011, 2012, 2014; Mosquera et al. 2018), TD6.2 was little affected by geological processes, so the composition and position derived from the archaeological remains are excellent for the interpretation of human settlement in Gran Dolina and the early settlements of Europe.

Supplementary Information The online version contains supplementary material available at https://doi.org/10.1007/s12520-021-01303-6.

Acknowledgments We want to express our gratitude to our colleagues from the Atapuerca Research Team for the hard work that is done year after year. Raquel Pérez Martínez has provided us with all the drawings of the trench and Grand Dolina. We have had the support of Efstathia Robakis in the English edition. We want to express our gratitude to the two anonymous reviewers and editor Dr. Stephen Shennan, for their willingness and time invested in improving the manuscript.

Authors' contribution Palmira Saladié: conceptualization, investigation, formal analysis, methodology, interpretation, interpretation, writing (original draft), review and editing

Antonio Rodríguez-Hidalgo: conceptualization, investigation, formal analysis, methodology, writing (original draft), review and editing

Manuel Domínguez-Rodrigo: conceptualization, methodology, and interpretation

Josep Vallverdú: conceptualization, investigation, stratigraphic description, interpretation, and review (original draft)

Marina Mosquera: investigation, formal analysis, review and funding acquisition

Andreu Ollé: investigation, formal analysis, review original draft and funding acquisition

Rosa Huguet: investigation, formal analysis, and review original draft

Isabel Cáceres: investigation, formal analysis, and review original draft

Juan Luis Arsuaga: investigation and funding acquisition

José Maria Bermúdez de Castro: investigation and funding acquisition

Eudald Carbonell: conceptualization, investigation, review original draft and funding acquisition

Funding information The Ministry of Science, Innovation and Universities (MICINN-FEDER) of the Spanish Government financed the research, project no. PGC2018-093925-B-C32 and project no. FJCI-037447-I (Subprograma Juan de la Cierva) and, also, the AGAUR (project no. 2017 SGR-1040) and the URV (project no. 2018PFR-URV-B2-91). IPHES research is framed in CERCA Programme/Generalitat de Catalunya. The funding for fieldwork came from the Cultural and Tourism Council of Castilla y León and the Atapuerca Foundation. This research was supported by the Spanish Ministry of Science and Innovation through the "María de Maeztu" excellence accreditation (CEX2019-000945-M).

References

Arche A (1989) Análisis de facies y cuencas sedimentarias. Sedimentología 1:13–49

Arnold LJ, Demuro M, Parés JM, Pérez-González A, Arsuaga JL, Bermúdez de Castro JM, Carbonell E (2015) Evaluating the suitability of extended-range luminescence dating techniques over early and Middle Pleistocene timescales: published datasets and case studies from Atapuerca, Spain. Quat Int 389:167–190

Arzarello M, Marcolini F, Pavia G, Pavia M, Petronio C, Petrucci M, Rook L, Sardella R (2007) Evidence of earliest human occurrence in Europe: the site of Pirro Nord (Southern Italy). Naturwissenschaften 94:107–112

Aslan A, Behrensmeyer AK (1996) Taphonomy and time resolution of bone assemblages in a contemporary fluvial system: The East Fork River, Wyoming. Palaios 11:411–421

Baddeley A, Rubak E, Turner R (2015) Spatial point patterns: methodology and applications with R. CRC Press

Behrensmeyer AK (1975) Taphonomy and paleoecology in the Hominid fossil record. Yearb Phys Anthropol 19:36–50

Behrensmeyer AK (1978) Taphonomic and ecologic information from bone weathering. Paleobiology 4:150–162

Behrensmeyer AK (1988) Vertebrate preservation in fluvial channels. Palaeogeogr Palaeoclimatol Palaeoecol 63:183–199

Berger GW, Pérez-González A, Carbonell E, Arsuaga JL, Bermúdez de Castro JM, Ku TL (2008) Luminescence chronology of cave sediments at the Atapuerca paleoanthropological site, Spain. J Hum Evol 55:300–311

Berman M, Diggle P (1989) Estimating weighted integrals of the second-order intensity of a spatial point process. J R Stat Soc Ser B Methodol 51:81–92

Bermúdez de Castro JM, Arsuaga JL, Carbonell E, Rosas A, Martínez I, Mosquera M (1997) A hominid from the lower Pleistocene of Atapuerca, Spain: possible ancestor to Neandertals and modern humans. Science 276:1392–1395

Bermúdez de Castro JM, Carbonell E, Cáceres I, Díez JC, Fernández-Jalvo Y, Mosquera M, Ollé A, Rodríguez J, Rodríguez XP, Rosas A, Rosell J, Sala R, Vergés JM, van der Made J (1999) The TD6 (Aurora stratum) hominid site. Final remarks and new questions. J Hum Evol 37:695–700

Bermúdez de Castro JM, Carbonell E, Gómez A et al (2006) Paleodemografía del hipodigma de fósiles de homininos del nivel TD6 de Gran Dolina (Sierra de Atapuerca, Burgos): estudio preliminar. Estudios 62:145–154

Bermúdez de Castro JM, Pérez-González A, Martinón-Torres M et al (2008) A new early Pleistocene hominin mandible from Atapuerca-TD6, Spain. J Hum Evol 55:729–735

Boaz NT, Behrensmeyer AK (1976) Hominid taphonomy: transport of human skeletal parts in an artificial fluviatile environment. Am J Phys Anthropol 45:53–60

Britt BB, Eberth DA, Scheetz RD, Greenhalgh BW, Stadtman KL (2009) Taphonomy of debris-flow hosted dinosaur bonebeds at Dalton Wells, Utah (Lower Cretaceous, Cedar Mountain Formation, USA). Palaeogeogr Palaeoclimatol Palaeoecol 280:1–22

Bromage TG (1984) Interpretation of scanning electron microscopic images of abraded forming bones surfaces. Am J Phys Anthropol 64: 161–178

Bunn HT (1983) Comparative analysis of modern bone assemblages from a San Hunter-Gatherer Camp in the Kalahari Desert, Botswana, and from a Spotted Hyena Den Near Nairobi, Kenia. In: Clutton-Brock J, Grigson C (eds) Animals and Archaeology: 1.- Hunters and Their Prey. British Archaeological Reports. International Series 163, Oxford, pp 143–148

Campaña I, Pérez-González A, Benito-Calvo A, Rosell J, Blasco R, de Castro JMB, Carbonell E, Arsuaga JL (2016) New interpretation of the Gran Dolina-TD6 bearing Homo antecessor deposits through sedimentological analysis. Sci Rep 6:34799

Campaña I, Benito-Calvo A, Pérez-González A, Ortega AI, Bermúdez de Castro JM, Carbonell E (2017) Pleistocene sedimentary facies of the Gran Dolina archaeo-paleoanthropological site (Sierra de Atapuerca, Burgos, Spain). Quat Int 433:68–84

Canals A, Vallverdú J, Carbonell E (2003a) New archaeo-stratigraphic data for the TD6 level in relation to Homo antecessor Lower Pleistocene at the site of Atapuerca, North-Central Spain. Geoarchaeology 18:481–504

Canals A, van der Made J, Sauceda I, Carbonell E (2003b) El conjunto paleontológico de la cueva de Maltravieso (Cáceres): un nuevo yacimiento del Pleistoceno. In: F.G. (ed) IX Reunión Nacional de Cuaternario. Consejería de Cultura, Principado de Asturias, Concejo de Candamo, Cajastur, AEQUA, Oviedo, pp 313–320

Carbonell E, de Castro B´d, JM JLA (1999a) Preface. J Hum Evol 37(3-4):309–311

Carbonell E, García-Antón MD, Mallol C et al (1999b) The TD6 level lithic industry from Gran Dolina, Atapuerca (Burgos, Spain): production and use. J Hum Evol 37:653–693

Carbonell E, Bermúdez de Castro JM, Arsuaga JL et al (2005) An Early Pleistocene hominin mandible from Atapuerca-TD6, Spain. Proc Natl Acad Sci U S A 102:5674–5678

Carbonell E, Cáceres I, Lozano M et al (2010) Cultural cannibalism as a paleoeconomic system in the European Lower Pleistocene: The case of level TD6 of Gran Dolina (Sierra de Atapuerca, Burgos, Spain). Curr Anthropol 51:539–549

Coard R (1999) One bone, two bones, wet bones, dry bones: transport potentials under experimental conditions. J Archaeol Sci 26:1369–1375

Díez JC, Fernández-Jalvo Y, Rosell J, Cáceres I (1999) Zooarchaeology and taphonomy of Aurora Stratum (Gran Dolina, Sierra de Atapuerca, Spain). J Hum Evol 37:623–652

Dodson P (1973) The significance of small bones in paleoecological interpretation. Rocky Mt Geol 12:15–19

Domingo MS, Martín-Perea D, Domingo L, Cantero E, Cantalapiedra JL, Yelo BAG, Cano ARG, Alcalde GM, Fesharaki O, Fernández MH (2017) Taphonomy of mammalian fossil bones from the debris-flow deposits of Somosaguas-North (Middle Miocene, Madrid Basin, Spain). Palaeogeogr Palaeoclimatol Palaeoecol 465:103–121

Domínguez-Rodrigo M (1997) Meat-eating by early hominids at the FLK 22 Zinjanthropus site, Olduvai Gorge (Tanzania): an experimental approach using cut-mark data. J Hum Evol 33:669–690

Domínguez-Rodrigo M, Cobo-Sánchez L (2017) A spatial analysis of stone tools and fossil bones at FLK Zinj 22 and PTK I (Bed I, Olduvai Gorge, Tanzania) and its bearing on the social organization of early humans. Palaeogeogr Palaeoclimatol Palaeoecol 488:21–34

Domínguez-Rodrigo M, Uribelarrea D, Santonja M, Bunn HT, García-Pérez A, Pérez-González A, Panera J, Rubio-Jara S, Mabulla A, Baquedano E, Yravedra J, Diez-Martín F (2014) Autochthonous anisotropy of archaeological materials by the action of water: experimental and archaeological reassessment of the orientation patterns at the Olduvai sites. J Archaeol Sci 41:44–68

Domínguez-Rodrigo M, Cobo-Sánchez L, Yravedra J, Uribelarrea D, Arriaza C, Organista E, Baquedano E (2018) Fluvial spatial taphonomy: a new method for the study of post-depositional processes. Archaeol Anthropol Sci 10:1769–1789

Domínguez-Rodrigo M, Baquedano E, Barba R, Uribelarrea D, Gidna A (2019a) The river that never was: Fluvial taphonomy at Olduvai Bed I and II sites and its bearing on early human behavior. Quat Int 526: 26–38. https://doi.org/10.1016/j.quaint.2019.09.038

Domínguez-Rodrigo M, Saladié P, Cáceres I, Huguet R, Yravedra J, Rodríguez-Hidalgo A, Patricia M, Antonio P, Juan M, Clara G, Aramendi J, Cobo-Sánchez L (2019b) Spilled ink blots the mind: A reply to Merrit et al. (2018) on subjectivity and bone surface modifications. J Archaeol Sci 102:80–86

Duval M, Grün R, Parés JM, Martín-Francés L, Campaña I, Rosell J, Shao Q, Arsuaga JL, Carbonell E, Bermúdez de Castro JM (2018) The first direct ESR dating of a hominin tooth from Atapuerca Gran Dolina TD-6 (Spain) supports the antiquity of Homo antecessor. Quat Geochronol 47:120–137

Falguères C, Bahain JJ, Yokoyama Y, Arsuaga JL, Bermudez de Castro JM, Carbonell E, Bischoff JL, Dolo JM (1999) Earliest humans in Europe: the age of TD6 Gran Dolina, Atapuerca, Spain. J Hum Evol 37:343–352

Fernández-Jalvo Y, Andrews P (2016) Atlas of Taphonomic Identifications. Vertebrate Paleobiology and Paleoanthropology Series. Springer doi 10:978–994

Fernández-Jalvo Y, Díez JC, Bermúdez de Castro JM et al (1996) Evidence of early cannibalism. Science 271:277–278

Fiorillo AR (1984) An introduction to the identification of trample marks. Curr Res in the Pleistocene 1:47–48

Ford D, Williams P (2007) Karst Hydrogeology and Geomorphology. John Wiley & Sons Ltd, New York

Gifford DP (1977) Observations of contemporary human settlements as an aid to archaeological interpretation. Ph. Dissertation, University of California, Ann Arbor: University Microfilms

Gil E, Hoyos M (1987) Contexto estratigráfico. In: Aguirre E, Carbonell E, Bermúdez de Castro JM (eds) El hombre fósil de Ibeas y el Pleistoceno de la Sierra de Atapuerca. Junta de Castilla y León, Soria, pp 47–54

Giusti D, Arzarello M (2016) The need for a taphonomic perspective in spatial analysis: Formation processes at the Early Pleistocene site of Pirro Nord (P13), Apricena, Italy. J Archaeol Sci Rep 8:235–249

Giusti D, Konidaris GE, Tourloukis V, Marini M, Maron M, Zerboni A, Thompson N, Koufos GD, Kostopoulos DS, Harvati K (2019) Recursive anisotropy: a spatial taphonomic study of the Early Pleistocene vertebrate assemblage of Tsiotra Vryssi, Mygdonia Basin, Greece. Boreas 48:713–730

Giusti D, Tourloukis V, Konidaris GE, Thompson N, Karkanas P, Panagopoulou E, Harvati K (2018) Beyond maps: patterns of formation processes at the Middle Pleistocene open-air site of Marathousa 1, Megalopolis basin, Greece. Quat Int 497:137–153

Hétu B (2004) Talús d'éboulis: Environnement et Histoire. In: Bertran P (ed) Dépôts de Pente Continentaux. Dynamique et Facies. Hors-série, Paris, pp 199–241

Hoyos M, Aguirre E (1995) El registro paleoclimático pleistoceno en la evolución del karst de Atapuerca (Burgos): El corte de gran dolina. Trab Prehist 52(2):31–45

Isaac G (1978) The food-sharing behaviour of proto-human hominids. Sci Am 238:90–108

Isaac G (1983) Aspects of human evolution. In: Bendall DS (ed) Evolution from Molecules to Men. Cambridge Universitt Press, Cambridge, pp 509–543

Jiménez-Jáimez V (2008) El ciclo formativo del registro arqueológico. Una alternativa a la dicotomía deposicional/posdeposicional. Zephyrus 62:125–137

LaMotta V, Schiffer MB (1999) Formation processes of house floor assemblages. In: Allison PM (ed) The archaeology of household activities. Routledge, London, pp 19–29

Lenoble A (2016) *Ruissellement et formation des sites préhistoriques : référentiel actualiste et exemples d'application au fossile*. BAR Publishing, Oxford

López-González F, Grandal-d'Anglade A, Vidal-Romaní JR (2006) Deciphering bone depositional sequences in caves through the study of manganese coatings. J Archaeol Sci 33:707–717

Luckman BH (2013) Processes, transport, deposition, and landforms: Rockfall. Treatise on Geomorphol:174–182

Marín J, Rodríguez-Hidalgo A, Vallverdú J, de Soler BG, Rivals F, Ramón Rabuñal J, Pineda A, Chacón MG, Carbonell E, Saladié P (2019) Neanderthal logistic mobility during MIS3: Zooarchaeological perspective of Abric Romaní level P (Spain). Quat Sci Rev 106033:225

Márquez B, Ollé A, Sala R, Vergès JM (2001) Perspectives méthodologiques de l'analyse fonctionnelle des ensembles lithiques du Pléistocène inférieur et moyen d'Atapuerca (Burgos, Espagne). Anthropologie 105:281–299

Martinón-Torres M, de Castro JMB, de Pinillos MM et al (2019) New permanent teeth from Gran Dolina-TD6 (Sierra de Atapuerca). The bearing of Homo antecessor on the evolutionary scenario of Early and Middle Pleistocene Europe. J Hum Evol 127:93–117

McPherron SP (2018) Additional statistical and graphical methods for analyzing site formation processes using artifact orientations. PLoS One 13:e0190195

Mosquera M, Ollé A, Rodríguez-Álvarez XP, Carbonell E (2018) Shedding light on the Early Pleistocene of TD6 (Gran Dolina, Atapuerca, Spain): The technological sequence and occupational inferences. PLoS One 13:e0190889

Nemec W, Steel RJ (1984) Alluvial and coastal conglomerates: their significant features and some comments on gravelly mass-flow deposits. In: Koster EH, Steel RJ (eds) Sedimentology of Gravels and Conglomerates. CSPG Special Publications, Canadian Society of Petroleum Geologists Memoir, pp 1–31

Pante MC, Blumenschine RJ (2010) Fluvial transport of bovid long bones fragmented by the feeding activities of hominins and carnivores. J Archaeol Sci 37:846–854

Parés JM, Pérez-González A (1995) Paleomagnetic age for hominid fossils at Atapuerca Archaeological site, Spain. Science 269:830–832

Parés JM, Pérez-González A (1999) Magnetochronology and stratigraphy at Gran Dolina section, Atapuerca (Burgos, Spain). J Hum Evol 37: 325–342

Parés JM, Arnold L, Duval M, Demuro M, Pérez-González A, Bermúdez de Castro JM, Carbonell E, Arsuaga JL (2013) Reassessing the age of Atapuerca-TD6 (Spain): new paleomagnetic results. J Archaeol Sci 40:4586–4595

Parés JM, Álvarez C, Sier M, Moreno D, Duval M, Woodhead JD, Ortega AI, Campaña I, Rosell J, Bermúdez de Castro JM, Carbonell E (2018) Chronology of the cave interior sediments at Gran Dolina archaeological site, Atapuerca (Spain). Quat Sci Rev 186:1–16

Parés JM, Campaña I, Duval M, Sier MJ, Ortega AI, López GI, Rosell J (2020) Comparing depositional modes of cave sediments using magnetic anisotropy. J Archaeol Sci 123:105241

Pérez-González A, Parés JM, Carbonell E, Aleixandre T, Ortega AI, Benito A, Martin Merino MÁ (2001) Géologie de la Sierra de Atapuerca et stratigraphie des remplissages karstiques de Galería et Dolina (Burgos, Espagne). Anthropologie 105:27–43

Petraglia MD, Nash DT (1987) The impact of fluvial processes on experimental sites. In: Natural formation processes and the archaeological record. BAR, pp 108–130

Petraglia MD, Potts R (1994) Water Flow and the Formation of Early Pleistocene Artifact Sites in Olduvai Gorge, Tanzania. J Anthropol Archaeol 13:228–254

Ripley BD (1976) The second-order analysis of stationary point processes. J Appl Probab 13:255–266

Ripley BD (1977) Modelling Spatial Patterns. J R Stat Soc Ser B Methodol 39:172–192

Ripley BD (1979) Tests of "Randomness" for Spatial Point Patterns. J R Stat Soc Ser B Methodol 41:368–374

Ripley BD (1988) Statistical inference for spatial processes. Cambridge University Press, Cambridge

Robert CP, Casella G (2004) Variable Dimension Models and Reversible Jump Algorithms. Springer Texts in Statistics 425–458

Rodríguez-Gómez G, Palmqvist P, Ros-Montoya S, Espigares MP, Martínez-Navarro B (2017) Resource availability and competition intensity in the carnivore guild of the Early Pleistocene site of Venta Micena (Orce, Baza Basin, SE Spain). Quat Sci Rev 164:154–167

Rogers RR, Kidwell SM (2007) A conceptual framework for the genesis and analysis of vertebrate skeletal concentrations. In: Rogers RR, Eberth DA, Fiorillo AR (eds) Bonebeds: Genesis, Analysis and Paleobiological significance. University of Chicago Press, Chicago, pp 1–63

Sala R (1997) Formes d'ús i criteris d'efectivitat en conjunts de mode 1 i mode 2: Anàlisis de les deformacions per ús dels instruments lítics del Plistocè inferior (TD6) i mitjà (TG11) de la Sierra d'Atapuerca. Ph.D. Dissertation, Universitat Rovira i Virgili, Tarragona

Saladié P (2009) Mossegades d'omnívors. Aproximació experimental i aplicació zooarqueològica als jaciments de la Sierra de Atapuerca. Ph. D. Dissertation, URV

Saladié P, Huguet R, Díez C, Rodríguez-Hidalgo A, Cáceres I, Vallverdú J, Rosell J, Bermúdez de Castro JM, Carbonell E (2011) Carcass

transport decisions in Homo antecessor subsistence strategies. J Hum Evol 61:425–446
Saladié P, Huguet R, Rodríguez-Hidalgo A, Cáceres I, Esteban-Nadal M, Arsuaga JL, Bermúdez de Castro JM, Carbonell E (2012) Intergroup cannibalism in the European Early Pleistocene: The range expansion and imbalance of power hypotheses. J Hum Evol 63:682–695
Saladié P, Rodríguez-Hidalgo A, Huguet R, Cáceres I, Díez C, Vallverdú J, Canals A, Soto M, Santander B, Bermúdez de Castro JM, Arsuaga JL, Carbonell E (2014) The role of carnivores and their relationship to hominin settlements in the TD6-2 level from Gran Dolina (Sierra de Atapuerca, Spain). Quat Sci Rev 93:47–66
Saladié P, Fernández P, Rodríguez-Hidalgo A, Huguet R, Pineda A, Cáceres I, Marín J, Vallverdú J, Carbonell E (2019) The TD6.3 faunal assemblage of the Gran Dolina site (Atapuerca, Spain): a late Early Pleistocene hyena den. Hist Biol 31:665–683
Sanders D, Ostermann M, Kramers J (2009) Quaternary carbonate-rocky talus slope successions (Eastern Alps, Austria): sedimentary facies and facies architecture. Facies 55:345–373
Schick KD (1984) Processes of Palaeolithic site formation: an experimental study. University of California, Berkeley
Schick KD (1986) Stone Age sites in the making: experiments in the formation and transformation of archaeological occurrences. British Archaeological Reports Ltd
Schick KD (1987) Experimentally-derived criteria for assessing hyrologic disturbance of archaeological sites. In: Nash DT, Petraglia (eds) Natural formation processes and the archaeological record. BAR International Series, pp 86–107
Schiffer MB (1983) Toward the identification of Formation Processes. Am Antiq 48:675–706
Schiffer MB (1987) Formation Processes of the Archaeological Record. University of Utah Press, Salt Lake City
Shipman P (1981) Life History of a Fossil. An introduction to taphonomy and paleoecology. Harvard University Press, Cambridge
Shipman P, Rose J (1983) Early hominid hunting, butchering, and carcass-processing behaviors: approaches to the fossil record. J Anthropol Archaeol 2:57–98
Stanford CB, Bunn H (2001) Meat-eating and human evolution. Oxford University Press, New York
Tanner LH, Hubert JF (1991) Basalt breccias and conglomerates in the Lower Jurassic McCoy Brook Formation, Fundy Basin, Nova Scotia; differentiation of talus and debris-flow deposits. J Sediment Res 61:15–27
Thompson CEL, Ball S, Thompson TJU, Gowland R (2011) The abrasion of modern and archaeological bones by mobile sediments: the importance of transport modes. J Archaeol Sci 38:784–793
Todd S (1996) Process deduction from fluvial sedimentary structures. In: Carling PA, Dawson MR (eds) Advances in Fluvial Dynamics and Stratigraphy. John Wiley, Chichester, pp 290–335
Toro-Moyano I, Martínez-Navarro B, Agustí J et al (2013) The oldest human fossil in Europe, from Orce (Spain). J Hum Evol 65:1–9
Vallverdú J, Courty MA, Carbonell E et al (2001) Les sédiments d'Homo antecessor de Gran Dolina (Sierra de Atapuerca, Burgos, Espagne). Interprétation micromorphologique des processus de formation et enregistrement paléoenvironnemental des sédiments. Anthropologie 105:45–71
Vallverdú J, Saladié P, Rosas A, Huguet R, Cáceres I, Mosquera M, Garcia-Tabernero A, Estalrrich A, Lozano-Fernández I, Pineda-Alcalá A, Carrancho Á, Villalaín JJ, Bourlès D, Braucher R, Lebatard A, Vilalta J, Esteban-Nadal M, Bennàsar ML, Bastir M, López-Polín L, Ollé A, Vergés JM, Ros-Montoya S, Martínez-Navarro B, García A, Martinell J, Expósito I, Burjachs F, Agustí J, Carbonell E (2014) Age and date for early arrival of the Acheulian in Europe (Barranc de la Boella, la Canonja, Spain). PLoS One 9:e103634
Voorhies M (1969) Taphonomy and population dynamics of early Pliocene vertebrate fauna, Knox County, Nebraska. Rocky Mountain Geology 8(Special Paper):1–69

Publisher's note Springer Nature remains neutral with regard to jurisdictional claims in published maps and institutional affiliations.